

$R_{D^{(*)}}$ IN CUSTODIAL WARPED SPACEMarcela Carena^{a,b}, Eugenio Megías^c, Mariano Quirós^{d,e}, Carlos Wagner^{b,f}^a *Fermi National Accelerator Laboratory, P. O. Box 500, Batavia, IL 60510, USA*^b *Enrico Fermi Institute and Kavli Institute for Cosmological Physics,
University of Chicago, Chicago, IL 60637, USA*^c *Departamento de Física Atómica, Molecular y Nuclear and
Instituto Carlos I de Física Teórica y Computacional, Universidad de Granada,
Avenida de Fuente Nueva s/n, 18071 Granada, Spain*^d *Institut de Física d'Altes Energies (IFAE) and BIST
Campus UAB, 08193, Bellaterra, Barcelona, Spain*^e *Department of Physics, University of Notre Dame
225 Nieuwland Hall, Notre Dame, IN 46556, USA*^f *HEP Division, Argonne National Laboratory, 9700 Cass Ave., Argonne, IL 60439, USA***Abstract**

Flavor physics experiments allow to probe the accuracy of the Standard Model (SM) description at low energies, and are sensitive to new heavy gauge bosons that couple to quarks and leptons in a relevant way. The apparent anomaly in the ratios of the decay of B -mesons into D -mesons and different lepton flavors, $R_{D^{(*)}} = \mathcal{B}(B \rightarrow D^{(*)}\tau\nu)/\mathcal{B}(B \rightarrow D^{(*)}\ell\nu)$ is particularly intriguing, since these decay processes occur at tree-level in the SM. Recently, it has been suggested that this anomaly may be explained by new gauge bosons coupled to right-handed currents of quarks and leptons, involving light right-handed neutrinos. In this work we present a well-motivated ultraviolet complete realization of this idea, embedding the SM in a warped space with an $SU(2)_L \otimes SU(2)_R \otimes U(1)_{B-L}$ bulk gauge symmetry. Besides providing a solution to the hierarchy problem, we show that this model, which has an explicit custodial symmetry, can explain the $R_{D^{(*)}}$ anomaly and at the same time allow for a solution to the $R_{K^{(*)}}$ anomalies, related to the decay of B -mesons into K -mesons and leptons, $R_{K^{(*)}} = \mathcal{B}(B \rightarrow K^{(*)}\mu\mu)/\mathcal{B}(B \rightarrow K^{(*)}ee)$. In addition, a model prediction is an anomalous value of the forward-backward asymmetry A_{FB}^b , driven by the $Z\bar{b}_R b_R$ coupling, in agreement with LEP data.

Contents

1	Introduction	3
2	The model	4
3	Generating $R_{D^{(*)}}$	11
4	Constraints	13
4.1	The coupling $Z\tau_R\tau_R$	15
4.2	Oblique observables	16
4.3	Flavor observables	19
4.4	Lepton flavor universality tests	21
4.5	LHC bounds	21
5	Predictions	24
5.1	The forward-backward asymmetry A_{FB}^b	24
5.2	The processes $B \rightarrow K\nu\nu$ and $B^+ \rightarrow K^+\tau^+\tau^-$	27
5.3	$R_{K^{(*)}}$	29
6	Conclusions	32
A	The KK-modes	34

1 Introduction

The Standard Model (SM) of particle physics provides an excellent description of all observables measured at collider experiments. The discovery of the Higgs boson [1, 2] is an evidence of the realization of the simplest electroweak symmetry breaking mechanism, based on the vacuum expectation value (VEV) of a Higgs doublet. This mechanism provides a moderate breakdown of the custodial $SU(2)_R$ symmetry that affects the gauge bosons only at the loop level. The predictions of the SM are also in agreement with precision electroweak observables, which show only loop-size departures from the tree-level gauge predictions [3].

Flavor physics experiments allow to further probe the accuracy of the SM predictions. While studying SM rare processes, these experiments become sensitive to heavy new physics coupled in a relevant way to quarks and leptons. Recently, the BABAR [4, 5], BELLE [6–10] and LHCb [11] experiments have measured the ratio of the decay of B -mesons into D -mesons and different lepton flavors,

$$R_{D^{(*)}} = \frac{\mathcal{B}(B \rightarrow D^{(*)}\tau\nu)}{\mathcal{B}(B \rightarrow D^{(*)}\ell\nu)}, \quad \ell = \mu, e. \quad (1.1)$$

These decay processes occur at tree-level in the SM, and therefore can only be affected in a relevant way by either light charged gauge bosons, or heavy ones strongly coupled to the SM fermion fields. Currently, the measurements of these experiments seem to suggest a deviation of a few tens of percent from the SM predictions, a somewhat surprising result in view of the absence of any clear LHC new physics signatures, or other similar deviations in other flavor physics experiment.

In particular, the presence of new $SU(2)$ gauge interactions affecting the left-handed neutrinos, which could provide an explanation of the new $R_{D^{(*)}}$ anomaly, is strongly restricted by the measurement of the branching ratio of the decay of B -mesons into K -mesons plus invisible signatures by the BELLE collaboration $\mathcal{B}(B \rightarrow K\nu\nu)$ [12–14]. Recently, it was proposed that a possible way of avoiding these constraints was to assume that the new gauge interactions were coupled to right-handed currents and the neutrinos are therefore right handed neutrinos [15, 16]. The right-handed neutral currents are then affected by right-handed quark mixing angles that are not restricted by current measurements, and provide the freedom to adjust the invisible decays to values consistent with current measurements.

In this work, we propose a well-motivated, ultraviolet complete, realization of the new gauge interactions coupled to the right handed currents, by embedding the SM in warped space, with a bulk gauge symmetry $SU(2)_L \otimes SU(2)_R \otimes U(1)_{B-L}$ [17–20]. This symmetry is broken to $SU(2)_L \otimes U(1)_Y$ in the ultraviolet brane, implying the absence of charged, W_R^\pm , and neutral, Z_R , gauge boson zero modes. *Third generation* quark and leptons are localized in the infrared-brane, where a Higgs bi-doublet provides the necessary

breakdown of the SM gauge symmetry, giving masses to quarks and leptons. Although there have been previous works on the flavor structure of warped extra dimensions with a $SU(2)_L \otimes SU(2)_R \times U(1)_X$ bulk gauge symmetry (see, for example, Refs. [21, 22]), those works put emphasis on rare Kaon and B -meson decays unrelated to $R_{D^{(*)}}$, that will also be analyzed in our work whenever relevant.

In this work, similarly to the previous proposal by the authors of Refs. [15, 16], the new $SU(2)_R$ gauge bosons provide an explanation of the $R_{D^{(*)}}$ anomaly, and the freedom in the right-handed mixing angles allows to avoid the invisible B decay and B -meson mixing constraints. On the other hand, our model depicts unique, attractive special features such as having an explicit custodial symmetry that protects it from large deviations in precision electroweak observables, and providing a solution of the hierarchy problem through the usual warped space embedding. Finally, although it is not the main aim of this article, the left-handed KK gauge bosons may be used to provide an explanation of the R_{K^*} anomalies in the way proposed in Refs. [23–25].

Our study is organized as follows. In Sec. 2 we present the model in some detail. In Sec. 3 we explain the solution to the $R_{D^{(*)}}$ anomaly. In Sec. 4 we discuss the existing experimental constraints on this model. In Sec. 5 we study the predictions of our model, including the forward-backward bottom asymmetry, the invisible decay of B mesons into K mesons, and the $b \rightarrow s\mu\mu$ observables, including $R_{K^{(*)}}$. Finally we reserve Sec. 6 for our conclusions and App. A for some technical details on the KK modes.

2 The model

Our setup will be a five dimensional (5D) model with metric (with the mostly minus signs convention) $g_{\mu\nu} = \exp(-ky)\eta_{\mu\nu}$, $g_{55} = -1$, in proper coordinates, and two branes, at the ultraviolet (UV) $y = 0$, and infrared (IR) $y = y_1$, regions, respectively [26]. The parameter k , close to the Planck scale, is related to the Anti de Sitter (AdS_5) curvature, and ky_1 has to be fixed by the stabilizing Goldberger-Wise (GW) mechanism [27] to a value of $\mathcal{O}(35)$, in order to solve the hierarchy problem.

The custodial model is based on the bulk gauge group [17–20]

$$SU(3)_c \otimes SU(2)_L \otimes SU(2)_R \otimes U(1)_X, \quad (2.1)$$

where $X \equiv B-L$, with 5D gauge bosons $(\mathcal{G}, W_L, W_R, X)$, and 5D couplings (g_c, g_L, g_R, g_X) ¹, respectively.

The breaking $SU(2)_R \otimes U(1)_X \rightarrow U(1)_Y$, where Y is the SM hypercharge with gauge boson B and coupling g_Y , is done in the UV brane by boundary conditions. Therefore the gauge fields (W_L^a, W_R^a, X) define $(W_L^a, W_R^{1,2}, B, Z_R)$, with (UV, IR) boundary conditions,

¹The 5D (g_5) and 4D (g_4) couplings are related by $g_4 = g_5/\sqrt{y_1}$.

as

$$W_L^a \ (a = 1, 2, 3), \quad (+, +) \quad (2.2)$$

$$B = \frac{g_X W_R^3 + g_R X}{\sqrt{g_R^2 + g_X^2}}, \quad (+, +) \quad (2.3)$$

$$W_R^{1,2}, \quad (-, +) \quad (2.4)$$

$$Z_R = \frac{g_R W_R^3 - g_X X}{\sqrt{g_R^2 + g_X^2}}. \quad (-, +) \quad (2.5)$$

The $SU(2)_L \otimes SU(2)_R$ symmetry is unbroken in the IR brane, where all composite states are localized, such that the *custodial* symmetry is exact. In App. A we present some technical details leading to the wave function, mass and coupling of the n th KK modes for both $(+, +)$ and $(-, +)$ boundary conditions. It is shown there that the difference for the KK mode masses m_n , and couplings, is tiny for the different boundary conditions, $(+, +)$ and $(-, +)$, and different electroweak symmetry breaking masses, and we will neglect it throughout this paper. In particular we will use the notation m_1 for the first KK mode mass of the different 5D gauge bosons after electroweak breaking: $(W_L^\pm, W_R^\pm, Z_R, Z_L, A)$.

The covariant derivative for fermions is

$$\not{D} = \not{\partial} - i \left[g_L \sum_{a=1}^3 \not{W}_L^a T_L^a + g_R \sum_{b=1}^2 \not{W}_R^b T_R^b + g_Y \not{B} Y + g_{Z_R} \not{Z}_R Q_{Z_R} \right] \quad (2.6)$$

where g_Y and g_{Z_R} are defined in terms of g_R and g_X as

$$g_Y = \frac{g_R g_X}{\sqrt{g_R^2 + g_X^2}}, \quad g_{Z_R} = \sqrt{g_R^2 + g_X^2}, \quad (2.7)$$

and the hypercharge Y and the charge Q_{Z_R} are defined by

$$Y = T_R^3 + Q_X, \quad Q_{Z_R} = \frac{g_R^2 T_R^3 - g_X^2 Q_X}{g_R^2 + g_X^2} \quad (2.8)$$

with $Q_X = (B - L)/2$.

Electroweak symmetry breaking is triggered in the IR brane by the bulk Higgs bi-doublet

$$\mathcal{H} = \begin{pmatrix} H_2^0 & H_1^+ \\ H_2^- & H_1^0 \end{pmatrix}, \quad Q_X = 0 \quad (2.9)$$

where the rows transform under $SU(2)_L$ and the columns under $SU(2)_R$. We will denote their VEVs as $\langle H_2^0 \rangle \equiv v_2/\sqrt{2}$ and $\langle H_1^0 \rangle \equiv v_1/\sqrt{2}$, so that we will introduce the angle β as, $\cos \beta = v_1/v_H$ and $\sin \beta = v_2/v_H$, with $v_H = \sqrt{v_1^2 + v_2^2}$. We will find it useful to add an extra Higgs bi-doublet

$$\Sigma = \begin{pmatrix} \Sigma^-/\sqrt{2} & \Sigma^0 \\ \Sigma^{--} & -\Sigma^-/\sqrt{2} \end{pmatrix}, \quad Q_X = -1 \quad (2.10)$$

with $\langle \Sigma^0 \rangle = v_\Sigma / \sqrt{2}$, whose usefulness will be justified later on in this paper.

After electroweak breaking, and rotating to the gauge boson mass eigenstates, one can re-write the covariant derivative as

$$\begin{aligned} \not{D} = & \not{\partial} - i g_L \left[\frac{1}{\sqrt{2}} W_L^\pm T_L^\pm + \frac{1}{\cos \theta_L} Z_L (T_L^3 - \sin^2 \theta_L Q) \right] - i g_L \sin \theta_L A Q \\ & - i g_R \left[\frac{1}{\sqrt{2}} W_R^\pm T_R^\pm + \frac{1}{\cos \theta_R} Z_R (T_R^3 - \sin^2 \theta_R Y) \right] \end{aligned} \quad (2.11)$$

where $\theta_L \equiv \theta_W$ is the usual weak mixing angle, the gauge boson $Z_L^\mu \equiv Z^\mu$, and θ_R is defined as

$$\cos \theta_R = \frac{g_R}{\sqrt{g_R^2 + g_X^2}}, \quad \sin \theta_R = \frac{g_X}{\sqrt{g_R^2 + g_X^2}} \quad (2.12)$$

with $T_{L,R}^\pm \equiv T_{L,R}^1 \pm i T_{L,R}^2$. Using g_R and g_Y , with $g_R > g_Y$, as independent parameters we can write

$$g_X = \frac{g_Y g_R}{\sqrt{g_R^2 - g_Y^2}}, \quad \sin \theta_R = \frac{g_Y}{g_R}, \quad \cos \theta_R = \frac{\sqrt{g_R^2 - g_Y^2}}{g_R} \quad (2.13)$$

As for fermions, left-handed (LH) ones are in $SU(2)_L$ bulk doublets as in the SM

$$Q_L^i = \begin{pmatrix} u_L \\ d_L \end{pmatrix}^i, \quad L_L^i = \begin{pmatrix} \nu_L \\ e_L \end{pmatrix}^i \quad (2.14)$$

where the index i runs over the three generations. On the other hand, as $SU(2)_R$ is a symmetry of the bulk, right-handed (RH) fermions should appear in doublets of $SU(2)_R$. However, as $SU(2)_R$ is broken by the orbifold conditions on the UV brane it means, for bulk right-handed fermions, that one component of the doublet must be even, under the orbifold \mathbb{Z}_2 parity, and has a zero mode, while the other component of the doublet must be odd, and thus without any zero mode. We thus have to double the SM right-handed fermions in the bulk.

The natural assignment is to assume in the bulk first and second (light) generation fermions:

$$U_R^I = \begin{pmatrix} u_R \\ d_R' \end{pmatrix}^I, \quad D_R^I = \begin{pmatrix} u_R' \\ d_R \end{pmatrix}^I, \quad E_R^I = \begin{pmatrix} \nu_R' \\ e_R \end{pmatrix}^I, \quad (I = 1, 2) \quad (2.15)$$

where only the unprimed fermions have zero modes, while third generation (heavy) fermions are localized on the IR brane and thus are in $SU(2)_R$ doublets as

$$Q_R^3 = \begin{pmatrix} t_R \\ b_R \end{pmatrix}, \quad L_R^3 = \begin{pmatrix} \nu_R \\ \tau_R \end{pmatrix} \quad (2.16)$$

Then only the third generation RH fermions interact in a significant way with the field W_R , and can give rise to a sizable $R_{D^{(*)}}$, as we will see.

We define the KK modes for gauge bosons as

$$A_\mu(x, y) = \sum_{n=0}^{\infty} \frac{f_A^n(y)}{\sqrt{y_1}} A_\mu(x) \quad (2.17)$$

normalized as

$$\int_0^{y_1} f_A^n f_A^m dy = y_1 \delta_{nm} \quad (2.18)$$

and such that the factor $1/\sqrt{y_1}$ in Eq. (2.17) is absorbed by the 5D gauge coupling in Eq. (2.11) to become the corresponding 4D gauge coupling. Similar definitions hold for KK modes of $Z_L(x, y)$ and $W_L(x, y)$, while for KK modes of $Z_R(x, y)$ and $W_R(x, y)$ the sum extends from $n = 1$.

From the covariant derivative (2.11) it is clear that the charged bosons W_L^\pm only interact with left-handed fermions, while W_R^\pm only interact with right handed fermions. The corresponding 4D Lagrangian can be written as

$$\frac{g_L}{\sqrt{2}} \sum_{f_L, f'_L} G_{f_L f'_L}^n \bar{f}_L W_L^n f'_L + \frac{g_R}{\sqrt{2}} \sum_{f_R, f'_R} G_{f_R f'_R}^n \bar{f}_R W_R^n f'_R \quad (2.19)$$

where, from now on, we are switching to the notation where g_L and g_R are the 4D couplings, and $G_{f_L, R f'_L, R}^n$ are the overlapping integrals of the fermion zero-mode profiles, $f_{L, R}(y) f'_{L, R}(y)$, with the gauge boson KK mode ones, $W_{L, R}^n(y)$. On the other hand, the neutral gauge bosons A , Z_L and Z_R interact with both chiralities, and we can thus define the 4D neutral current Lagrangian for KK modes as

$$\mathcal{L}_n = \frac{g_L}{\cos \theta_L} \sum_f G_f^n \bar{f} (g_{Z_L f f} Z_L^n + g_{A f f} A^n) f + \frac{g_R}{\cos \theta_R} \sum_f g_{Z_R f f} G_f^n \bar{f} Z_R^n f \quad (2.20)$$

where for simplicity we have omitted the chirality indices and G_f^n is the overlapping integral of zero modes fermion profiles, $f_{L, R}^2(y)$, with the one of the (neutral) gauge boson KK modes. The 4D coupling of photons with fermions is defined as $g_{A f f} = \sin \theta_L \cos \theta_L Q$, the couplings of fermions with Z_R are given by

$$\begin{aligned} g_{Z_R u_R u_R} &= \frac{1}{2} - \frac{2}{3} \sin^2 \theta_R & g_{Z_R u_L u_L} &= -\frac{1}{6} \sin^2 \theta_R \\ g_{Z_R d_R d_R} &= -\frac{1}{2} + \frac{1}{3} \sin^2 \theta_R & g_{Z_R d_L d_L} &= -\frac{1}{6} \sin^2 \theta_R \\ g_{Z_R \nu_R \nu_R} &= \frac{1}{2} & g_{Z_R \nu_L \nu_L} &= \frac{1}{2} \sin^2 \theta_R \\ g_{Z_R e_R e_R} &= -\frac{1}{2} + \sin^2 \theta_R & g_{Z_R e_L e_L} &= \frac{1}{2} \sin^2 \theta_R, \end{aligned} \quad (2.21)$$

and with Z_L by

$$\begin{aligned}
g_{Z_L u_R u_R} &= -\frac{2}{3} \sin^2 \theta_L & g_{Z_L u_L u_L} &= \frac{1}{2} - \frac{2}{3} \sin^2 \theta_L \\
g_{Z_L d_R d_R} &= \frac{1}{3} \sin^2 \theta_L & g_{Z_L d_L d_L} &= -\frac{1}{2} + \frac{1}{3} \sin^2 \theta_L \\
g_{Z_L \nu_R \nu_R} &= 0 & g_{Z_L \nu_L \nu_L} &= \frac{1}{2} \\
g_{Z_L e_R e_R} &= \sin^2 \theta_L & g_{Z_L e_L e_L} &= -\frac{1}{2} + \sin^2 \theta_L .
\end{aligned} \tag{2.22}$$

The 5D Yukawa couplings for RH quarks localized on the IR brane are

$$Y_Q^{i3} Q_{Li} \mathcal{H} Q_{R3} + \tilde{Y}_Q^{i3} Q_{Li} \tilde{\mathcal{H}} Q_{R3} \tag{2.23}$$

where $\tilde{\mathcal{H}} = i\sigma_2 \mathcal{H}^* i\sigma_2$, and for the bulk RH quarks

$$Y_Q^{iI} Q_{Li} \mathcal{H} U_{Ri} + \hat{Y}_Q^{iI} Q_{Li} \mathcal{H} D_{Ri} + \tilde{Y}_Q^{iI} Q_{Li} \tilde{\mathcal{H}} U_{Ri} + \hat{\tilde{Y}}_Q^{iI} Q_{Li} \tilde{\mathcal{H}} D_{Ri} \tag{2.24}$$

so that the 4D Yukawa matrices are given by

$$\begin{aligned}
Y_{iI}^u &= \left(\sin \beta Y_Q - \cos \beta \tilde{Y}_Q \right)_{iI} F(c_{u_L^i}, c_{u_R^I}), \\
Y_{i3}^u &= \left(\sin \beta Y_Q - \cos \beta \tilde{Y}_Q \right)_{i3} F_3(c_{u_L^i}),
\end{aligned} \tag{2.25}$$

and

$$\begin{aligned}
Y_{iI}^d &= \left(\cos \beta \hat{Y}_Q - \sin \beta \hat{\tilde{Y}}_Q \right)_{iI} F(c_{d_L^i}, c_{d_R^I}), \\
Y_{i3}^d &= \left(\cos \beta Y_Q - \sin \beta \tilde{Y}_Q \right)_{i3} F_3(c_{d_L^i})
\end{aligned} \tag{2.26}$$

In the previous expressions the 4D Yukawa matrices $Y_{ij}^{u,d}$ contain the 5D Yukawa matrices $Y_Q, \tilde{Y}_Q, \hat{Y}_Q, \hat{\tilde{Y}}_Q$ times the integrals overlapping the 5D profiles of the corresponding fermions with the profile of the Higgs acquiring vacuum expectation value, $h(y) \propto e^{\alpha k y}$.

$$\begin{aligned}
F(c_L, c_R) &= \frac{\sqrt{2(\alpha-1)(1-2c_L)(1-2c_R)}}{\alpha - c_L - c_R} \frac{e^{(\alpha-c_L-c_R)ky_1} - 1}{\sqrt{[e^{2(\alpha-1)ky_1} - 1][e^{(1-2c_L)ky_1} - 1][e^{(1-2c_R)ky_1} - 1]}} \\
F_3(c_L) &= \frac{\sqrt{2(\alpha-1)(1-2c_L)}}{\sqrt{[e^{2(\alpha-1)ky_1} - 1][e^{(1-2c_L)ky_1} - 1]}} \frac{e^{(\alpha-1/2-c_L)ky_1}}{1}
\end{aligned} \tag{2.27}$$

where $c_{L,R}$ are the fermion bulk mass parameters and we have assumed that $\alpha > c_L + c_R$. The parameter α has to be larger than two, to solve the hierarchy problem, and in our computations we will fix $\alpha = 2$.

Similarly for RH leptons in the IR brane

$$Y_L^{i3} L_{Li} \mathcal{H} L_{R3} + \tilde{Y}_L^{i3} L_{Li} \tilde{\mathcal{H}} L_{R3} \quad (2.28)$$

and for bulk RH leptons

$$Y_L^{iI} L_L^i \mathcal{H} N_R^I + \hat{Y}_L^{iI} L_L^i \mathcal{H} E_R^I + \tilde{Y}_L^{iI} L_L^i \tilde{\mathcal{H}} N_R^I + \hat{\tilde{Y}}_L^{iI} L_L^i \tilde{\mathcal{H}} E_R^I, \quad (2.29)$$

where we have added the bulk first and second generation right-handed neutrino doublets

$$N_R^I = \begin{pmatrix} \nu_R \\ e_R' \end{pmatrix}^I, \quad I = (1, 2). \quad (2.30)$$

The Yukawa couplings for charged leptons are then given by

$$\begin{aligned} Y_{i3}^e &= (\cos \beta Y_L - \sin \beta \tilde{Y}_L)_{i3} F_3(c_{e_L^i}), \\ Y_{iI}^e &= (\cos \beta \hat{Y}_L - \sin \beta \hat{\tilde{Y}}_L)_{iI} F(c_{e_L^i}, c_{e_R^I}) \end{aligned} \quad (2.31)$$

and for neutrinos, by

$$\begin{aligned} Y_{iI}^\nu &= (\sin \beta Y_L - \cos \beta \tilde{Y}_L)_{iI} F(c_{\nu_L^i}, c_{\nu_R^I}) \\ Y_{i3}^\nu &= (\sin \beta Y_L - \cos \beta \tilde{Y}_L)_{i3} F_3(c_{\nu_L^i}) \end{aligned} \quad (2.32)$$

In the presence of a non-zero vacuum expectation value of the Σ field, we shall define

$$\tan \theta_\Sigma = \frac{v_\Sigma}{v_H}, \quad (2.33)$$

where $v = \sqrt{v_H^2 + v_\Sigma^2}$. In the decoupling limit, $H_1 = \cos \theta_\Sigma \cos \beta h - \sin \beta H - \sin \theta_\Sigma \cos \beta H_\Sigma$ and $H_2 = \cos \theta_\Sigma \sin \beta h + \cos \beta H - \sin \theta_\Sigma \sin \beta H_\Sigma$, while the neutral component of the Σ field, $\Sigma^0 = \sin \theta_\Sigma h + \cos \theta_\Sigma H_\Sigma$. The SM-like Higgs boson is induced by excitations of the field $h = \sin \theta_\Sigma \Sigma^0 + \cos \theta_\Sigma (\cos \beta H_1 + \sin \beta H_2)$, while the excitations induced by the orthogonal combinations H and H_Σ are supposed to lead to heavy neutral states, decoupled from the low energy theory. Since quarks and leptons only couple to the field \mathcal{H} , the masses are proportional to v_H and therefore the Yukawa couplings must be enhanced by a factor $(\cos \theta_\Sigma)^{-1}$ with respect to the value they would obtain in the absence of the Σ field.

In order to avoid strong constraints from lepton flavor violating processes, as e.g. $\mu \rightarrow e\gamma$, $\mu \rightarrow eee$, or $\mu - e$ conversion, we will assume that for charged leptons the interaction and mass eigenstate bases coincide, and therefore, hereafter, that the matrix Y^e is diagonal. This can be obtained by imposing a $U(1)^3$ flavor symmetry in the lepton sector broken only by the tiny effects due to the neutrino masses [28].

For neutrinos propagating in the bulk, one can obtain realistic values of their masses by adopting one of the proposed solutions for theories with warped extra dimensions [29–33]. In our scenario, however, neutrinos localized on the IR brane, as is the case with the right-handed neutrinos $\nu_{\tau,R}$, couple in a relevant way to the Higgs and tend to acquire masses of the same order as the charge lepton masses. This can be seen from the fact that the Yukawa couplings in Eq. (2.32) will provide a Dirac mass to the third generation neutrinos $m_D \bar{\nu}_L \nu_R + h.c.$. Therefore, in order to obtain realistic masses we will assume a double seesaw scenario [34]. We shall first concentrate on the example of third generation neutrinos. In order to realize this mechanism, we will introduce a Higgs H_R , transforming as $(1, 2, -1/2)$ under $SU(2)_L \otimes SU(2)_R \otimes U(1)_X$, which spontaneously breaks $SU(2)_R \times U(1)_X \rightarrow U(1)_Y$, when its neutral, hyperchargeless, component gets a vacuum expectation value v_R , as well as a localized fermion singlet $(1, 1, 0)$, S_L , which provides the Dirac mass $m'_D \bar{S}_L \nu_R + h.c.$, where $m'_D = Y_R v_R / \sqrt{2}$. Finally, we can also write down a Majorana mass term as $M S_L S_L$. Therefore the mass matrix in the basis (ν_L, ν_R^c, S_L) can be written as

$$\mathcal{M}_\nu = \begin{pmatrix} 0 & m_D & 0 \\ m_D & 0 & m'_D \\ 0 & m'_D & M \end{pmatrix} \quad (2.34)$$

In the limit where $m'_D \gg m_D \gg M$ there is a mass eigenstate $\nu_0 \simeq \nu_L$ with a mass $m_{\nu_0} \simeq (m_D/m'_D)^2 M$ (which is obviously massless in the limit where $M = 0$), and an approximate Dirac spinor $\nu_1 = (\nu_R^c - S_L, -\nu_R + S_L^c)^T / \sqrt{2}$, with a mass $m_{\nu_1} \simeq \sqrt{m_D^2 + m'^2_D}$. This mechanism has been dubbed in the literature, double seesaw [34]. The double seesaw mechanism allows for acceptable masses for the left- and right-handed neutrinos without extreme fine-tuning of the Yukawa couplings. For instance, for $m_D \simeq 1$ MeV, $m'_D \simeq 100$ MeV and $M = \mathcal{O}(1)$ KeV, one obtains a mostly left-handed neutrino of mass of order 0.1 eV, and an additional pseudo-Dirac neutrino, containing ν_R , of mass of order 100 MeV. Such masses are enough to accommodate the value of $R_{D(*)}$ without any sizable kinematic suppression.

The above mechanism can be easily generalized to give mass to the three generations of neutrinos. As suggested before, we will consider in the bulk the two RH neutrino doublets N_R^I and add two singlets S_L^I , while the third generation right-handed leptons and the singlet S_L^3 are as before localized in the IR brane. States transform under the flavor symmetry group $U(1)^3 = U(1)_{L_e} \otimes U(1)_{L_\mu} \otimes U(1)_{L_\tau}$, where the lepton number is defined as $L \equiv L_e + L_\mu + L_\tau$, in Tab. 1

The quantum numbers in Tab. 1 lead to the off-diagonal entries in Eq. (2.34). In particular $(m'_D)_{ij}$, defined as

$$\begin{aligned} (m'_D)_{iI} &= Y_R^{iI} \bar{S}^i \tilde{H}_R N_R^I + h.c. \\ (m'_D)_{i3} &= Y_R^{i3} \bar{S}^i \tilde{H}_R L_R^3 + h.c. \end{aligned} \quad (2.35)$$

is a diagonal matrix, while also the matrix $(m_D)_{ij}$ is diagonal as the bi-doublet \mathcal{H} does not carry any lepton number. Moreover we will introduce the non-diagonal Majorana

	L_e	L_μ	L_τ	L
N_R^1	1	0	0	1
N_R^2	0	1	0	1
L_R^3	0	0	1	1
H_R	1/3	1/3	1/3	1
S_L^1	2/3	-1/3	-1/3	0
S_L^2	-1/3	2/3	-1/3	0
S_L^3	-1/3	-1/3	2/3	0

Table 1: *Leptonic quantum numbers of fields involved in neutrino masses.*

mass matrix for singlets as $M_{ij}S_L^iS_L^j$ which will constitute a soft breakdown of the global symmetry $U(1)_{L_e} \otimes U(1)_{L_\mu} \otimes U(1)_{L_\tau}$, by the small M mass matrix elements, leading to the neutrino mass matrix [34]

$$m_\nu = m_D \frac{1}{m'_D} M \left(m_D \frac{1}{m'_D} \right)^T \quad (2.36)$$

which should describe the neutrino masses and PMNS mixing angles [3].

3 Generating $R_{D(*)}$

Only fermion doublets localized on the IR brane, with both non-vanishing components, will interact with W_R . Then we can write the 4D charged current Lagrangian, Eq. (2.19), in the mass eigenstate fermion basis as

$$\mathcal{L} = \frac{g_R}{\sqrt{2}} \sum_{n=1}^{\infty} \{ \bar{u}_R (V_{u_R}^\dagger G^n V_{d_R}) \tilde{W}_R^n d_R + \bar{\tau}_R \tilde{W}_R^n G^n \nu_{\tau_R} \} \quad (3.1)$$

where the matrix form has been used. The coupling matrix G^n can be approximated by

$$G^n \equiv \text{diag} (G_1^n, G_2^n, G_3^n) \quad (3.2)$$

where $G_{1,2}^n \ll G_3^n = f_{W_R}^n(y_1)$, and $f_{W_R}^n(y)$ is the normalized wave-function of the Kaluza-Klein modes of W_R^n (see App. A). After integration of the KK modes we can write down the effective Lagrangian

$$\mathcal{L}_{eff} = -\frac{4G_F}{\sqrt{2}} V_{cb} C_\tau (\bar{c}_R \gamma^\mu b_R) (\bar{\tau}_R \gamma_\mu \nu_{\tau_R}) \quad (3.3)$$

which has been normalized to the SM contribution, where the Wilson coefficient is given by

$$C_\tau = \sum_n \left(\frac{g_R}{2} G_3^n \frac{v}{m_n} \right)^2 \frac{(V_{u_R}^\dagger)_{23}}{V_{cb}} \simeq 1.45 \left(\frac{g_R}{2} G_3 \frac{v}{m_1} \right)^2 \frac{(V_{u_R}^\dagger)_{23}}{V_{cb}} \quad (3.4)$$

where $G_3 \equiv G_3^1$ and m_1 are the coupling and mass of the first KK mode, and the pre-factor 1.45 takes into account the contribution of the whole tower.

The Wilson coefficient C_τ contributes to the process $b \rightarrow c\tau\bar{\nu}_\tau$ and thus to the ratio

$$\frac{R_{D^{(*)}}}{R_{D^{(*)}}^{SM}} = 1 + |C_\tau|^2 \quad (3.5)$$

and the best fit value to experimental data is given by $C_\tau \simeq 0.46$ [16]². Using this value there is a relation between the ratio $(V_{u_R}^\dagger)_{23}/V_{cb}$ and the mass m_1 given by

$$m_1 \simeq \frac{0.64}{\sin\theta_R} \left(\frac{(V_{u_R}^\dagger)_{23}}{V_{cb}} \right)^{1/2} \text{ TeV} \quad (3.6)$$

so that the element $(V_{u_R}^\dagger)_{23}$ as a function of $\sin\theta_R$ and the mass m_1 is given in Fig. 1.

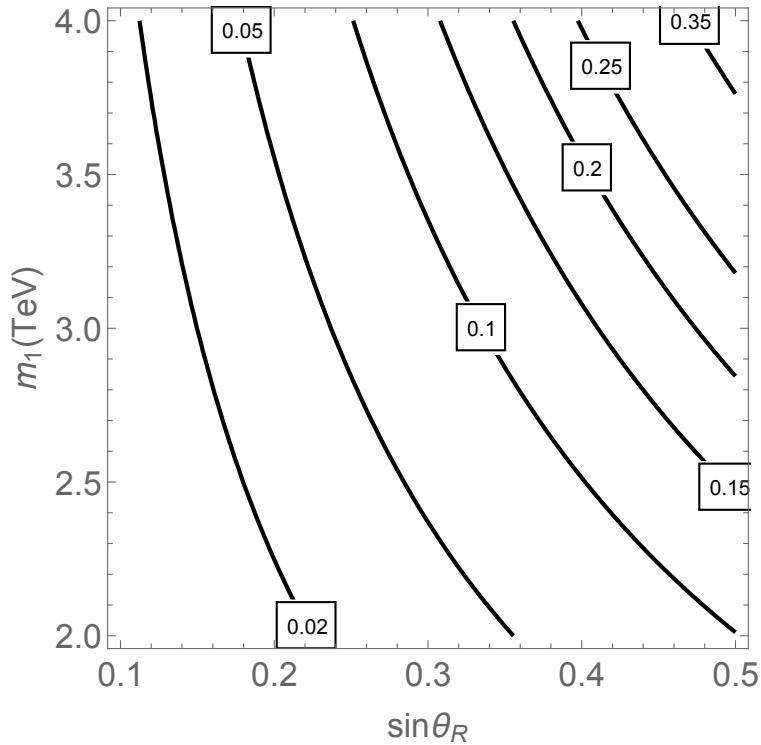


Figure 1: *Contour lines of $(V_{u_R}^\dagger)_{23}$ in the plane $(\sin\theta_R, m_1)$ as fixed from the best fit value to the experimental data for $R_D^{(*)}$.*

In principle the anomaly in the branching ratio $\mathcal{B}(B \rightarrow D^{(*)}\tau_R\bar{\nu}_R)$ might give rise to a large contribution to the branching fraction $\mathcal{B}(D_s \rightarrow \tau\bar{\nu}) \simeq 0.05$ from the process

²In Ref. [16] the best fit value $C_\tau \simeq 0.46$ is shown to be consistent with the experimental bound $\mathcal{B}(B_c \rightarrow \tau\bar{\nu}) < 0.05$ [35].

$\bar{s}c \rightarrow \tau_R^+ \nu_R$, which is mediated by the KK modes W_R^n . However since c_R and s_R are in the bulk, and in different $SU(2)_R$ doublets, they couple to W_R^n only via mixing with the third generation quarks. This implies that this contribution is further suppressed by a factor $(V_{d_R})_{32}$ which, as we will see, is restricted to be small to satisfy the constraints on Δm_{B_s} . Thus, no significant contribution to the branching ratio $\mathcal{B}(D_s \rightarrow \tau \nu)$ is obtained.

Similarly, in this model one would also expect an excess in the observable

$$R(J/\Psi) = \frac{B(B_c^+ \rightarrow J/\Psi \tau^+ \nu_\tau)}{B(B_c^+ \rightarrow J/\Psi \mu^+ \nu_\mu)}. \quad (3.7)$$

The LHCb experiment has recently provided a result on this observable, showing an excess of the order of 2σ above the SM expected value, $R(J/\Psi)_{\text{SM}} \simeq 0.25\text{--}0.28$, Ref. [36], with large errors

$$R(J/\Psi) = 0.71 \pm 0.25. \quad (3.8)$$

Theoretical analyses of this observable [37, 38] confirm this anomaly and show it to be governed by the same operator as the one governing $R_{D^{(*)}}$. In our particular model, we have

$$\frac{R(J/\Psi)}{R(J/\Psi)_{\text{SM}}} = 1 + |C_\tau|^2. \quad (3.9)$$

Given the value of $R(J/\Psi)_{\text{SM}}$, the measured value of this ratio is about 2.6 ± 1 . Hence, the value of C_τ obtained above to explain $R_{D^{(*)}}$ can only slightly ameliorate this anomaly, and one should wait for more accurate experimental measurements of $R(J/\Psi)$ before further discussion of this issue.

4 Constraints

In this section we will examine the main constraints in processes which are related to $R_{D^{(*)}}$, and where the strong coupling of the third generation RH quarks and leptons to KK modes plays a significant role. To do that one has to compute the mixing between the electroweak gauge bosons W_L^\pm and Z_L and the KK modes using the effective Lagrangian.

We can easily compute the effective description of the Lagrangian, with mixing terms $W_L W_{L,R}^n$ and $Z_L Z_{L,R}^n$, generated by the vacuum expectation values of the bulk Higgs bi-doublets \mathcal{H} and Σ as well as the Higgs doublet H_R in the representation $(1, 2)$, with VEV $\langle H_R \rangle = (v_R, 0)^T$, and with $Q_X = -1/2$. These are induced from the kinetic terms in the 5D Lagrangian as

$$\mathcal{L}^{\text{GH}} = \text{tr} |g_L W_L^a T_L^a \mathcal{H} - g_R \mathcal{H} W_R^a T_R^a|^2 + \text{tr} |g_L W_L^a T_L^a \Sigma - g_R \Sigma W_R^a T_R^a - g_X X \Sigma|^2 \quad (4.1)$$

$$+ |g_R H_R W_R^a T_R^a - \frac{1}{2} g_X X H_R|^2 \quad (4.2)$$

where we are using the fact that T_L^a acts on the bi-doublets rows and T_R^a on the bi-doublets columns.

A straightforward calculation gives for the 4D quadratic Lagrangian for the gauge boson n -th KK modes

$$\begin{aligned} \mathcal{L}_n^G = & g_L^2 \frac{v^2}{4} W_L W_L + \frac{g_L^2}{\cos^2 \theta_L} \frac{v^2}{8} Z_L Z_L \\ & + \frac{v^2}{4} G_3^n r_h(\alpha) \left\{ g_L^2 (W_L W_L^n + h.c.) - \frac{2v_1 v_2}{v^2} g_L g_R (W_L W_R^n + h.c.) \right\} \\ & + \frac{v^2}{4} G_3^n r_h(\alpha) \left\{ \frac{g_L^2}{\cos^2 \theta_L} Z_L Z_L^n + \frac{g_L g_R}{\cos \theta_L \cos \theta_R} [2 \sin^2 \theta_\Sigma - \cos^2 \theta_R] Z_L Z_R^n \right\} \end{aligned} \quad (4.3)$$

where $v^2 = v_1^2 + v_2^2 + v_\Sigma^2$, the first two terms provide the W_L and Z_L -masses, and we have introduced the function $r_h(\alpha)$ which depends on the localization in the bulk of the h Higgs direction acquiring a vacuum expectation value. In fact for a Higgs localized in the IR brane, $\alpha \rightarrow \infty$, one gets $r_h \simeq 1$, while for a Higgs localized towards the UV brane $\alpha \leq 1$ one gets $r_h \simeq 0$. For $\alpha = 2$ the Higgs is sufficiently localized towards the IR brane to solve the hierarchy problem, and we shall use this value in the rest of in this article, leading to a factor $r_h \simeq 0.68$.

Another important effect for analyzing the relevant constraints, in the presence of composite, and partly composite, fermions f , is that in our model the effective operators

$$\mathcal{O}_{ft_R} = (\bar{f} \gamma^\mu f) (\bar{t}_R \gamma_\mu t_R) \quad (4.4)$$

are induced, with Wilson coefficients given by

$$C_{ft_R} = - \sum_n \left(\frac{G_3^n}{m_n} \right)^2 r_f(c_f) \left[\frac{g_L^2}{\cos^2 \theta_L} (g_{Aff} g_{At_R t_R} + g_{Z_L f f} g_{Z_L t_R t_R}) + \frac{g_R^2}{\cos^2 \theta_R} g_{Z_R f f} g_{Z_R t_R t_R} \right]. \quad (4.5)$$

In the above, we have introduced the function $r_f(c_f)$ as

$$r_f(c_f) \equiv G_f^n(c_f) / G_3^n,$$

where $G_f^n(c_f)$ is the overlapping integral of fermion zero mode profiles, for the given value of the c_f parameter, and the gauge boson KK mode profile. In particular, for IR localized fermions, which could be considered as the limiting case where $c_f \rightarrow -\infty$, it turns out that $\lim_{c_f \rightarrow -\infty} r_f(c_f) = 1$. The Wilson coefficients trigger a one-loop modification of the $Z_L \bar{f} f$ couplings, through a top-quark loop diagram followed by emission of the Z_L gauge boson [39], which in turn induces the modification of the corresponding $Z_L \bar{f} f$ coupling. In particular, for the relevant cases we will analyze here $f = \tau_R, b_R, b_L, \mu_L$ are the composite (b_R, τ_R), or partly composite (b_L, μ_L), fermions.

4.1 The coupling $Z\tau_R\tau_R$

As the τ_R lepton is localized on the IR brane, and it couples strongly to the KK modes, the main constraint will be the modification of the coupling $Z_L\tau_R\tau_R$, defined as

$$\mathcal{L}_{Z\tau_R\tau_R} = \frac{g_L}{\cos\theta_L} \bar{\tau}_R \not{Z}_L (g_{Z_L\tau_R\tau_R} + \delta g_{Z_L\tau_R\tau_R}) \tau_R, \quad (4.6)$$

where the term $\delta g_{Z_L\tau_R\tau_R}$ is constrained by the global fit to the experimental data of Ref. [40] as

$$\delta g_{Z_L\tau_R\tau_R} = (0.42 \pm 0.62) \times 10^{-3}. \quad (4.7)$$

The term $\delta g_{Z_L\tau_R\tau_R}$ in Eq. (4.6) is generated at the tree level by the mixing $Z_{L,R}^n Z_L$ induced by the Higgs vacuum expectation value, and through radiative corrections using

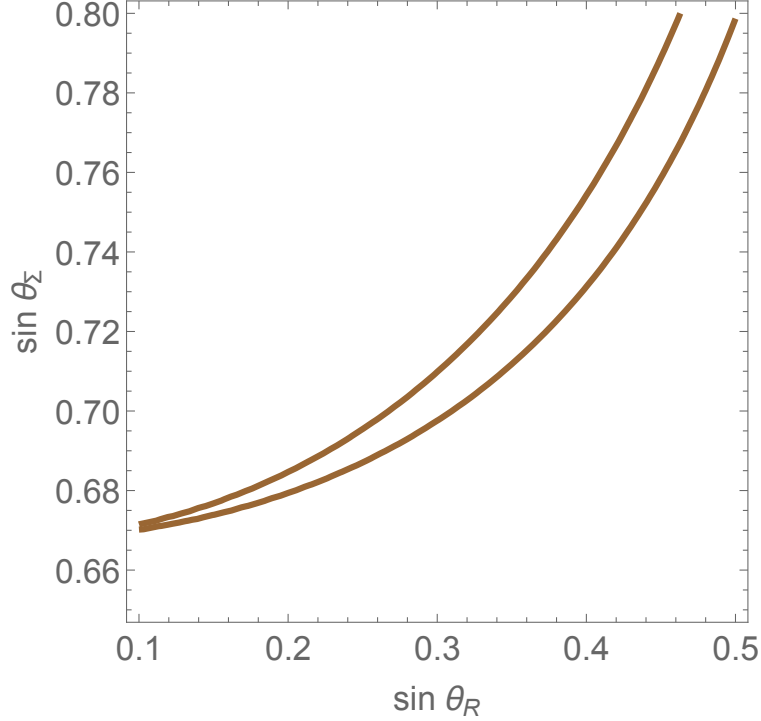


Figure 2: *The region between the (brown) solid lines is allowed by the best fit to $\delta g_{Z_L\tau_R\tau_R}$ for $m_1 = 3$ TeV.*

the effective operator

$$\mathcal{O}_{\tau_R t_R} = (\bar{\tau}_R \gamma^\mu \tau_R) (\bar{t}_R \gamma_\mu t_R) \quad (4.8)$$

with Wilson coefficient given by Eq. (4.5). Using now the mixing terms from Eq. (4.3)

and the couplings from Eqs. (2.21) and (2.22) we can write

$$\begin{aligned} \delta g_{Z_L \tau_R \tau_R} = & \sum_n \left(\frac{g_R v G_3^n}{2m_n} \right)^2 \left\{ \frac{r_h(\alpha)}{\cos^2 \theta_R} \left[\sin^2 \theta_\Sigma (1 - 2 \sin^2 \theta_R) - \frac{1}{2} \cos^2 \theta_R \right] \right. \\ & \left. + \frac{3h_t^2}{4\pi^2} \log \frac{m_1}{m_t} \left[\frac{2}{3} \sin^2 \theta_R + \frac{1}{\cos^2 \theta_R} \left(\frac{1}{2} - \sin^2 \theta_R \right) \left(\frac{1}{2} - \frac{2}{3} \sin^2 \theta_R \right) \right] \right\}, \end{aligned} \quad (4.9)$$

where the first line comes from the contribution of the KK gauge bosons through mixing effects and the second line is the radiative contribution from the top quark loop³ induced by the operator (4.8). The coupling h_t is the SM top-Yukawa coupling, defined by

$$m_t \equiv h_t v / \sqrt{2}, \quad (4.10)$$

which is therefore related to the Y_{33}^u coupling defined in Eq. (2.25) by

$$h_t = \cos \theta_\Sigma Y_{33}^u. \quad (4.11)$$

In order to determine the KK-mode contribution we use the condition (3.4) on $R_{D(*)}$ and get the allowed region in the plane $(\sin \theta_\Sigma, \sin \theta_R)$ shown in Fig. 2, where we are assuming $m_1 = 3$ TeV. Fig. 2 shows that the constraint on $\delta g_{Z_L \tau_R \tau_R}$ puts a lower bound on $\sin \theta_\Sigma$, which is given by

$$\sin \theta_\Sigma = \frac{v_\Sigma}{v} \gtrsim 0.67, \quad (4.12)$$

and in particular excludes the value $\sin \theta_\Sigma = 0$, i.e. it requires the introduction of the Higgs bi-doublet Σ .

4.2 Oblique observables

In these theories the T -parameter, defined as,

$$\alpha_{EM}(m_Z)T = \left[\frac{\Pi_{WW}(0)}{m_W^2} - \frac{\Pi_{ZZ}(0)}{m_Z^2} \right], \quad (4.13)$$

is protected by the custodial symmetry in the bulk only in the case when $\tan \beta = 1$ and $\sin \theta_\Sigma = 0$.

In general, there may be relevant contributions to the precision electroweak observables induced by the mixing of the gauge boson zero modes with the KK modes, as given by Eq. (4.3), as well as loop corrections induced by top loop corrections. In fact in a similar way as the operator (4.4) is generated by exchange of (A^n, Z_L^n, Z_R^n) KK modes, the operator

$$(H^\dagger i D_\mu H)(\bar{t}_R \gamma^\mu t_R) \quad (4.14)$$

³We have done the calculation using DimReg and the \overline{MS} renormalization scheme.

is generated by the mixing of Z_L with KK modes in (4.3) followed by the exchange of (Z_L^n, Z_R^n) KK modes coupled to the top quark. The radiative correction to the T parameter is obtained after closing the top-loop, and by emission of a Z_L -gauge boson from it.

There are also loop contributions involving fermionic KK modes, but in a scenario in which the right handed third generation fermions are localized on the infrared brane, they strongly depend on the localization of the left handed third generation quarks (see, for example, Refs. [41–43]). In particular, these loop corrections are strongly suppressed when the left-handed third generation quarks are localized close to the IR brane, or in the presence of sizable quark brane kinetic terms. Moreover, unlike the mixing between gauge KK n -modes and gauge zero modes, which is enhanced for IR brane localized fermions by $\sim |G_3^n| = \sqrt{2ky_1}$, the mixing between fermion KK n -modes and fermion zero modes is $\sim G_3^n/\sqrt{ky_1}$, so that the loop corrections to the T parameter are not volume-enhanced, while they are suppressed by the mass of the heavy fermions and by loop factors. Hence, in this work, we shall concentrate on the relevant corrections to flavor physics observables induced by the gauge boson mixing, and the inter-generational mixing of the right-handed quarks, as well as by the top loop corrections we have just described from the operator (4.14). These corrections to the precision electroweak observables are well defined within our framework, and are strongly correlated with our proposed solution to $R_{D(*)}$.

We can easily compute the contributions to the T -parameter induced by the mixing of the zero mode gauge bosons with the KK modes by using the effective description of the Lagrangian, with mixing terms $W_L W_{L,R}^n$ and $Z_L Z_{L,R}^n$, from Eq. (4.3), and at one-loop from the effective operator (4.14). Working to lowest order, $\mathcal{O}(v^4)$, in Higgs insertions, we obtain the result

$$\begin{aligned} \alpha T = r_h(\alpha) \sum_n \left(\frac{g_R v G_3^n}{2m_n} \right)^2 & \left\{ r_h(\alpha) \left[\cos^2 2\beta - 4 \sin^2 \theta_\Sigma \left(1 - \frac{\sin^2 \theta_\Sigma}{\cos^2 \theta_R} \right) \right. \right. \\ & \left. \left. + \sin^2 2\beta \sin^2 \theta_\Sigma (2 - \sin^2 \theta_\Sigma) \right] \right. \\ & \left. - \frac{3h_t^2}{2\pi^2} \log \frac{m_1}{m_t} \left[-\frac{2}{3} \sin^2 \theta_R + \frac{1}{\cos^2 \theta_R} (2 \sin^2 \theta_\Sigma - \cos^2 \theta_R) \left(\frac{1}{2} - \frac{2}{3} \sin^2 \theta_R \right) \right] \right\} \end{aligned} \quad (4.15)$$

where the first two lines is the tree-level result and the third line the radiative correction induced at one-loop by the mixing between the tree-level (4.3) and one-loop (4.14) operators.

Using now the expression fitting the value of $R_{D(*)}$, we can obtain the allowed regions for the T parameter in the $(\sin \theta_\Sigma, \sin \theta_R)$ plane, fixing the values of m_1 and $\tan \beta$. In Fig. 3, in addition to the $\delta g_{Z_L \tau_R \tau_R}$ bounds from Fig. 2, we show the regions allowed by the T parameter experimental bounds at the 95% confidence level [3]

$$T = 0.07 \pm 0.12, \quad (4.16)$$

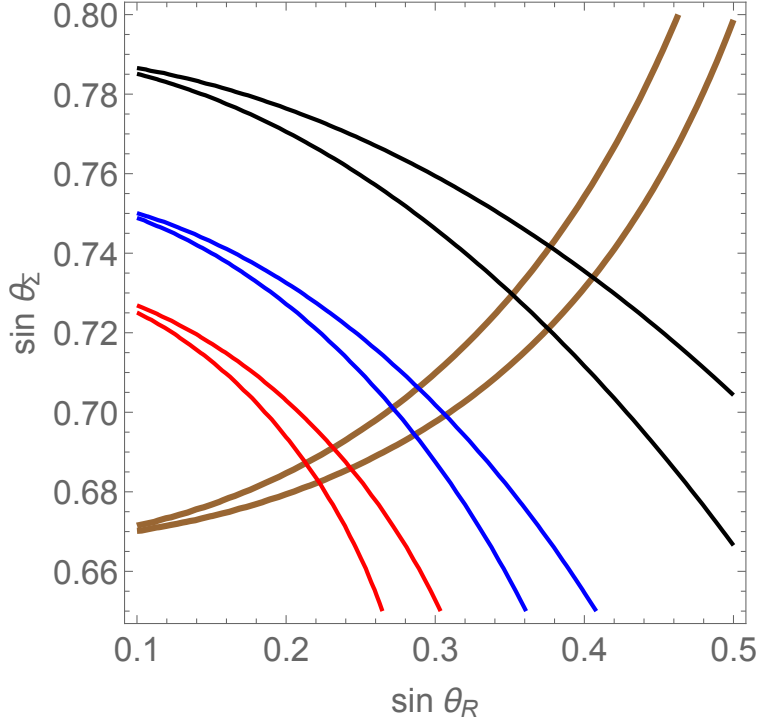


Figure 3: The region between the solid lines is allowed by $\delta g_{Z_L \tau_R \tau_R}$ (brown lines, as obtained in Fig. 2) and by the 95 % C.L. bound on the T parameter, for $m_1 = 3$ TeV and $\tan \beta = 1$ (black lines), $\tan \beta = 3$ (blue lines) and $\tan \beta = 5$ (red lines).

for $m_1 = 3$ TeV and several values of $\tan \beta = 1, 3, 5$. The value $T = 0$ is a middle line inside every band. In order to reduce the value of the Yukawa coupling Y_{33}^u , Eq. (2.25), we should consider values of $\tan \beta > 1$. The intersection of the $\delta g_{Z_L \tau_R \tau_R}$ allowed band with the T parameter allowed band for $\tan \beta = 1$ (solid brown and black lines, respectively), define the upper bounds on $\sin \theta_R$ and $\sin \theta_\Sigma$ in the regime we are considering as,

$$\sin \theta_R \lesssim 0.4, \quad \sin \theta_\Sigma \lesssim 0.75. \quad (4.17)$$

As for the S and U parameters, they are defined in our theory as

$$\alpha_{EM}(m_Z)S = 4 \sin^2 \theta_L \cos^2 \theta_L \Pi'_{ZZ}(0) \quad (4.18)$$

$$\alpha_{EM}(m_Z)(S + U) = 4 \sin^2 \theta_L \Pi'_{WW}(0) \quad (4.19)$$

which, using the effective description of Eq. (4.3), can be cast as

$$\alpha_{EM}(m_Z)S = -\frac{2r_h^2(\alpha)}{ky_1} \sum_n \left(\frac{vg_R G_3^n}{2m_n} \right)^4 \sin^2 \theta_R \cos^2 \theta_L \left[\frac{\sin^2 \theta_R}{\sin^2 \theta_L} + \frac{(2 \sin^2 \theta_\Sigma - \cos^2 \theta_R)^2}{\cos^2 \theta_R} \right] \quad (4.20)$$

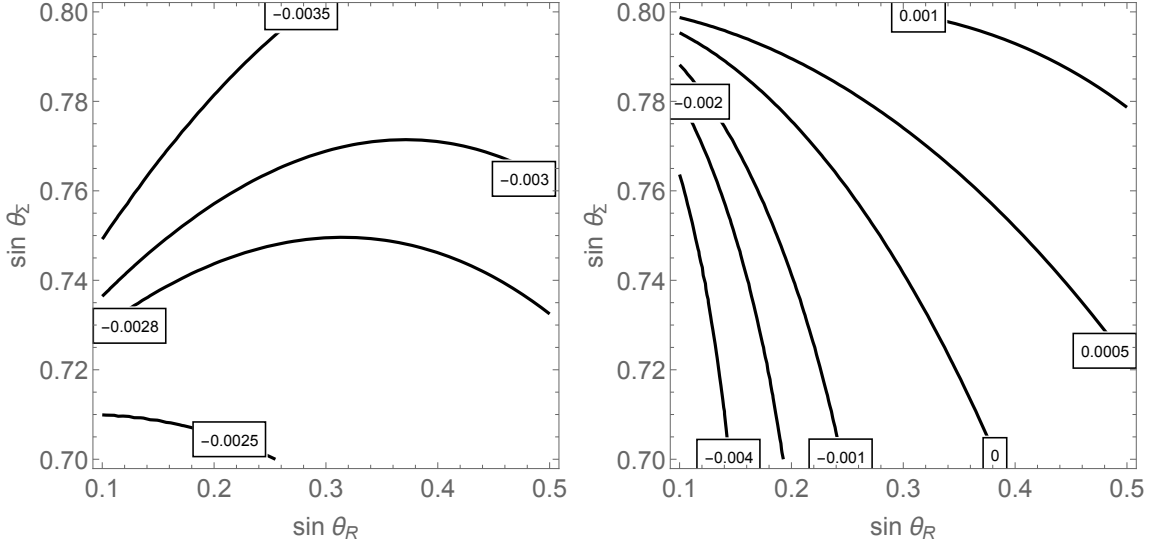


Figure 4: *Contour lines of S (left panel) and U (right panel) for the case $m_1 = 3$ TeV and $\tan \beta = 2$.*

and

$$\alpha_{EM}(m_Z)(S + U) = -\frac{2r_h^2(\alpha)}{ky_1} \sum_n \left(\frac{vg_R G_3^n}{2m_n} \right)^4 \sin^2 \theta_R \cos^4 \theta_L \left[\frac{\sin^2 \theta_R}{\sin^2 \theta_L} + \frac{\sin^2 2\beta}{\cos^2 \theta_L} \cos^4 \theta_\Sigma \right]. \quad (4.21)$$

where, as their tree level values is so small we are neglecting its crossing with the radiative corrections induced by the operator (4.14).

After applying the constraint from the $R_{D^{(*)}}$ anomaly, fixing the value of the KK mass, $m_1 = 3$ TeV, and $\tan \beta = 2$, the S and U counters are depicted in Fig. 4. It follows from this figure that the predicted values are consistent with the experimental constraint [3]

$$S = 0.02 \pm 0.10, \quad U = 0.00 \pm 0.09 \quad (4.22)$$

in all the parameter region. Similar small values of S and U are obtained for other values of $\tan \beta$.

4.3 Flavor observables

New physics contribution to $\Delta F = 2$ observables appears mainly from exchange of KK gluons. The leading flavor violating couplings of the KK gluons \mathcal{G}_μ^n involving RH down and up quarks is given by

$$\mathcal{L}_s = g_s (V_{u_R}^\dagger)_{i3} (V_{u_R})_{3j} \bar{u}_R^i \mathcal{G}_3^n G_3^m u_R^j + g_s (V_{d_R}^\dagger)_{i3} (V_{d_R})_{3j} \bar{d}_R^i \mathcal{G}_3^n G_3^m d_R^j. \quad (4.23)$$

After integrating out the gluon KK modes we obtain a set of $\Delta F = 2$ dimension six operators. In particular, the most constrained operators are those given by

$$\mathcal{L}_{eff} = C_{sd}(\bar{s}_R\gamma^\mu d_R)^2 + C_{cu}(\bar{c}_R\gamma^\mu u_R)^2 + C_{bd}(\bar{b}_R\gamma^\mu d_R)^2 + C_{bs}(\bar{b}_R\gamma^\mu s_R)^2 \quad (4.24)$$

where the Wilson coefficients are given by

$$C_{sd} = \frac{g_s^2}{6} \left[(V_{d_R}^\dagger)_{23} (V_{d_R})_{31} \right]^2 \sum_n \left(\frac{G_3^n}{m_n} \right)^2 \quad (4.25)$$

$$C_{cu} = \frac{g_s^2}{6} \left[(V_{u_R}^\dagger)_{23} (V_{u_R})_{31} \right]^2 \sum_n \left(\frac{G_3^n}{m_n} \right)^2 \quad (4.26)$$

$$C_{bd} = \frac{g_s^2}{6} [(V_{d_R})_{31}]^2 \sum_n \left(\frac{G_3^n}{m_n} \right)^2 \quad (4.27)$$

$$C_{bs} = \frac{g_s^2}{6} \left[(V_{d_R}^\dagger)_{23} \right]^2 \sum_n \left(\frac{G_3^n}{m_n} \right)^2, \quad (4.28)$$

where $(V_{u_R}^\dagger)_{23}$ is constrained by $R_{D(*)}$, see Fig. 1. If, for simplicity, we assume real matrices V_{u_R} and V_{d_R} (no CP violation in the right-handed sector) the Wilson coefficients C_{sd} , C_{cu} , C_{bd} and C_{bs} are constrained from Δm_K , Δm_D , Δm_{B_d} and Δm_{B_s} , respectively, as [44, 45]

$$C_{sd} < 9 \times 10^{-7} \text{ TeV}^{-2}, \quad (4.29)$$

$$C_{cu} < 5.6 \times 10^{-7} \text{ TeV}^{-2}, \quad (4.30)$$

$$C_{bd} < 2.3 \times 10^{-6} \text{ TeV}^{-2}, \quad (4.31)$$

$$C_{bs} < 5 \times 10^{-5} \text{ TeV}^{-2}. \quad (4.32)$$

Operators involving third generation quarks, although providing weaker bounds on the Wilson coefficients, are very constraining as they contain the element $(V_{d_R}^\dagger)_{33} \simeq 1$. In particular the bounds on C_{bd} and C_{bs} , Eqs. (4.31) and (4.32), provide bounds on $(V_{d_R})_{31}$ and $(V_{d_R}^\dagger)_{23}$, respectively, as

$$|(V_{d_R}^\dagger)_{13}| \lesssim 1.1 \times 10^{-3} \left(\frac{m_1}{3 \text{ TeV}} \right), \quad |(V_{d_R}^\dagger)_{23}| \lesssim 5.2 \times 10^{-3} \left(\frac{m_1}{3 \text{ TeV}} \right). \quad (4.33)$$

Using now the bounds in Eq. (4.33) we can bound the element C_{sd} as

$$C_{sd} < 4.5 \times 10^{-11} \left(\frac{m_1}{3 \text{ TeV}} \right)^2 \text{ TeV}^{-2}, \quad (4.34)$$

which is a stronger bound than Eq. (4.29). Moreover, from the definition of C_{cu} in Eq. (4.26) and the corresponding bound (4.30), we can fix an upper bound on the element $(V_{u_R})_{31}$ using the value of $(V_{u_R}^\dagger)_{23}$ provided by $R_{D(*)}$. The result is plotted in Fig. 5 as a function of $\sin \theta_R$.

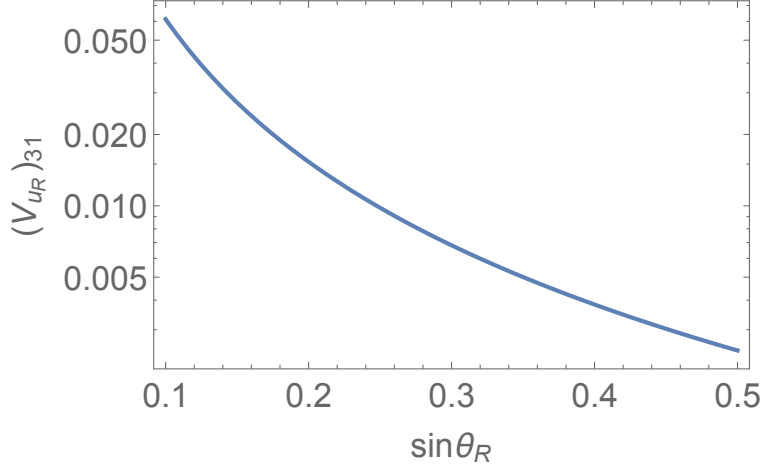


Figure 5: Upper bound on $(V_{u_R})_{31}$ as a function of $\sin \theta_R$ from condition (4.30) for $m_1=3$ TeV, using the value of $(V_{u_R}^\dagger)_{23}$ provided by $R_{D^{(*)}}$.

4.4 Lepton flavor universality tests

There are two processes where lepton flavor universality has been tested to hold with a high accuracy. The first one is the ratio

$$R_{D^{(*)}}^{\mu/e} = \frac{\mathcal{B}(B \rightarrow D^{(*)} \mu \bar{\nu}_\mu)}{\mathcal{B}(B \rightarrow D^{(*)} e \bar{\nu}_e)} \quad (4.35)$$

which is constrained by experimental data to be $R_{D^{(*)}}^{\mu/e} \lesssim 1.02$ [46]. In our model, the process $\Gamma(b \rightarrow c W_R^* \rightarrow c \ell \bar{\nu}_\ell) = 0$, for $\ell = (\mu, e)$, since only the third generation leptons couple to W_R . Hence, it follows that $R_{D^{(*)}}^{\mu/e} = R_{D^{(*)}}^{\mu/e}|_{SM} \simeq 1$ and the experimental bound is satisfied.

The second process is

$$R_\mu^{\tau/\ell} = \frac{\mathcal{B}(\tau \rightarrow \ell \nu_\tau \bar{\nu}_\ell) / \mathcal{B}(\tau \rightarrow \ell \nu_\tau \bar{\nu}_\ell)_{SM}}{\mathcal{B}(\mu \rightarrow e \nu_\mu \bar{\nu}_e) / \mathcal{B}(\mu \rightarrow e \nu_\mu \bar{\nu}_e)_{SM}}, \quad (\ell = \mu, e) \quad (4.36)$$

which is constrained by experimental data to be $R_\mu^{\tau/\mu} = 1.0022 \pm 0.0030$ and $R_\mu^{\tau/e} = 1.0060 \pm 0.0030$. It turns out that the contribution to these processes from W_R , $\mathcal{B}(\tau \rightarrow \nu_\tau W_R^* \rightarrow \nu_\tau \ell \bar{\nu}_\ell)$ and similarly $\mathcal{B}(\mu \rightarrow \nu_\mu W_R^* \rightarrow \nu_\mu \ell \bar{\nu}_\ell)$ is negligible for the same reason as before, and hence the deviation of $R_\mu^{\tau/\ell}$ with respect to the SM values is also negligible, in good agreement with these measurements.

4.5 LHC bounds

The first neutral KK resonance X^1 ($X = Z_L, Z_R, A$) can be produced on-shell at LHC in Drell-Yan processes $\sigma(b\bar{b} \rightarrow X^1)$, followed by decays $X^1 \rightarrow f\bar{f}$ where $f = \tau_R, b_R, t_R$. The

production cross-section times branching ratio can be written as

$$\sum_X \sigma(pp \rightarrow X^1) \times \mathcal{B}(X^1 \rightarrow f\bar{f}) = \frac{1}{9} g_R^2 2k y_1 f(m_1) \left[\sin^2 \theta_R \sin^2 \theta_L \mathcal{B}(Z_L^1 \rightarrow f\bar{f}) + \frac{1}{\cos^2 \theta_R} (3/2 - \sin^2 \theta_R)^2 \mathcal{B}(Z_R^1 \rightarrow f\bar{f}) + \sin^2 \theta_R \cos^2 \theta_L \mathcal{B}(A^1 \rightarrow f\bar{f}) \right] \quad (4.37)$$

where $f(m_1)$ is the production cross-section for unit coupling obtained by **MadGraph v5** [47].

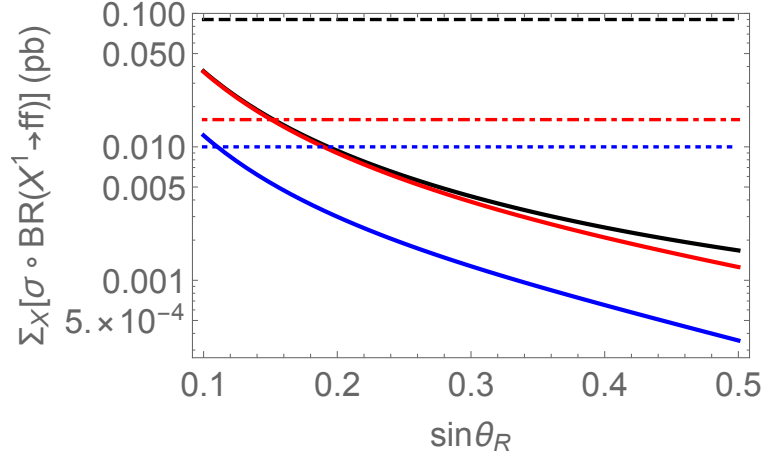


Figure 6: Plot of $\sum_X \sigma \times \mathcal{B}(X^1 \rightarrow \bar{f}f)$ as a function of $\sin \theta_R$, for $m_1 = 3$ TeV and $f = b_R$ (upper black solid line), $f = t_R$ (middle red solid line) and $f = \tau_R$ (lower blue solid line). Horizontal lines correspond to the 95% CL experimental upper bounds from the ATLAS experiment for $f = b_R$ (upper dashed line), for $f = t_R$ (middle dot-dashed red line) and $f = \tau_R$ (lower dotted blue line).

Our model prediction for $\sum_X \sigma(pp \rightarrow X^1) \times \mathcal{B}(X^1 \rightarrow \bar{f}f)$ is given by the upper, middle and lower solid lines of Fig. 6 for $f = b_R, t_R, \tau_R$, respectively. We compare them with the experimental 95% CL upper bounds from the corresponding processes, which are given by the dot-dashed (red), dashed (black) and dotted (blue) horizontal lines from the ATLAS experiment on $\sigma \times \mathcal{B}(Z' \rightarrow \bar{t}t)$ [48], $\sigma \times \mathcal{B}(Z' \rightarrow \bar{b}b)$ [49] and $\sigma \times \mathcal{B}(Z' \rightarrow \tau\tau)$ [50] for $m_{Z'} = 3$ TeV, respectively. As can be seen from Fig. 6 only the process $\sigma \times \mathcal{B}(Z' \rightarrow \bar{t}t)$ puts a significant bound on our model, of $\sin \theta_R \gtrsim 0.15$ for $m_1 = 3$ TeV, as we are assuming.

In a similar way the first charged KK resonance W_R^1 can be produced on-shell at the LHC in the process $\sigma(b\bar{c} \rightarrow W_R^1)$, followed by the decays $W_R \rightarrow \tau_R \nu_{\tau_R}, t_R \bar{b}_R$, that assuming that there are no exotic fermions localized in the IR brane, yield branching ratios around 1/4 and 3/4, respectively. In our model the production cross sections times

branching-ratio is

$$\sigma(pp \rightarrow W_R^1) \times \mathcal{B}(W_R^1 \rightarrow \tau_R \nu_{\tau_R}) \simeq \frac{g_R^2}{8} G_3^2 (V_{u_R}^\dagger)_{23}^2 g(m_1) \quad (4.38)$$

where $g(m_1)$ is the production cross-section for unit coupling obtained by **MadGraph v5** [47]⁴. Our model prediction for $\sigma(pp \rightarrow W_R) \times \mathcal{B}(W_R \rightarrow \tau_R \nu_{\tau_R})$ is given in Fig. 7, from where it follows that the model prediction is below the ATLAS 95% CL experimental upper bound $\sigma(pp \rightarrow W_R^1) \times \mathcal{B}(W_R^1 \rightarrow \tau_R \nu_{\tau_R})_{exp} \lesssim 0.0035$ pb [51] by a factor of order of a few.

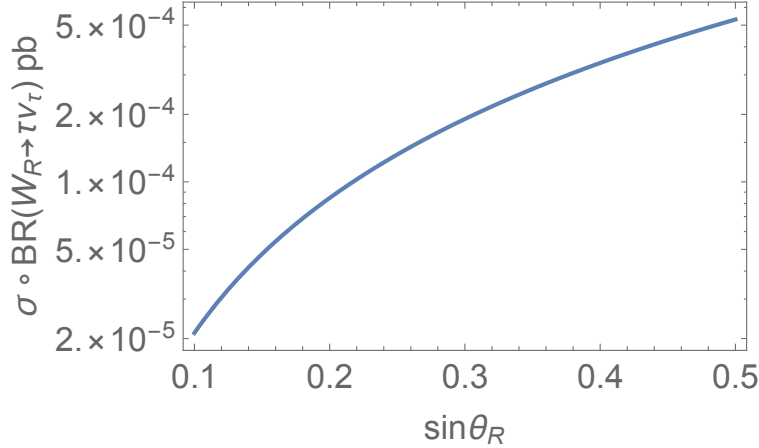


Figure 7: Plot of $\sigma(pp \rightarrow W_R^1) \times \mathcal{B}(W_R^1 \rightarrow \tau_R \nu_{\tau_R})$ as a function of $\sin \theta_R$, for $m_1 = 3$ TeV and the values of $(V_{u_R}^\dagger)_{23}$ required for the solution to the $R_D^{(*)}$ anomaly.

In the previous analyses we did not take into account the width of resonances. While the width (with respect to its mass m_1) of the KK photon A^1 is around ~ 0.24 , those of the other resonances depend on the angle $\sin \theta_R$. For instance, in the range $0.35 \lesssim \sin \theta_R \lesssim 0.5$ the Z_L^1 width varies between 0.05 and 0.08, while those of Z_R^1 and W_R^1 are generically $\mathcal{O}(1)$. For the case of broad resonances, as is the case of the Z_R^1 and W_R^1 resonances, we expect that the effect of the width can affect the production cross-section (due to possible KK mode superpositions) as well as the experimental bounds (due to the absence of a clear resonance). Recent ATLAS studies [48] show that bounds on the cross-sections for the case of broad resonances are affected by factors of order a few, while the cross-section predictions are also affected by similar factors. Hence, although a detailed experimental and theoretical analysis would be necessary to determine the precise bounds on the gauge boson KK mode masses, they are expected to be of the same order as the ones shown in Figs. 6 and 7.

Finally there are also strong constraints on the mass of KK gluons \mathcal{G}^1 from the cross-section $\sigma(pp \rightarrow \mathcal{G}^1) \times \mathcal{B}(\mathcal{G}^1 \rightarrow t\bar{t})$ from the ATLAS experimental analysis in Ref. [48].

⁴We thank Xiaoping Wang for help in the computation of these cross sections.

As the resonance \mathcal{G}^1 is a broad one, both the experimental results and the theoretical calculation of the production cross sections should be re-analyzed to get reliable bounds on the mass of the KK gluons. However, a simple way of relaxing the bounds is introducing brane kinetic terms for the $SU(3)$ gauge bosons, in particular in the IR brane. This theory has been analyzed in Refs. [52, 53], where it is shown that, even for small coefficients in front of the brane kinetic terms, the coupling of the KK modes \mathcal{G}^n to IR localized fermions decreases very fast while the mass of the modes m_n increases. Both facts going in the same directions, the bounds on KK gluons can be easily avoided. As the strong sector does not interfere with the electroweak one $SU(2)_L \otimes SU(2)_R \otimes U(1)_X$, the presence of brane kinetic terms will not affect our mechanism for reproducing the $R_{D^{(*)}}$ anomaly. Moreover in the presence of brane kinetic terms for $SU(3)$ gauge bosons the flavor bounds in Sec. 4.3 should be subsequently softened, an analysis that, to be conservative, we are not considering in this paper.

5 Predictions

In this section we will present some predictions of our theory consistent with the experimental value of $R_{D^{(*)}}$ and all the previously analyzed experimental constraints.

5.1 The forward-backward asymmetry A_{FB}^b

We shall study the shifts in the couplings $g_{Z_L b_{L,R} b_{L,R}}$, parametrized as

$$g_{Z_L b_{L,R} b_{L,R}} = g_{Z_L b_{L,R} b_{L,R}}^{SM} + \delta g_{Z_L b_{L,R} b_{L,R}}. \quad (5.1)$$

The shift of these couplings induce an anomalous modification of the forward-backward bottom asymmetry, conventionally defined as

$$A_{FB}^b = \frac{3}{4} A_{LR}^e \left(\frac{g_{Z_L b_L b_L}^2 - g_{Z_L b_R b_R}^2}{g_{Z_L b_L b_L}^2 + g_{Z_L b_R b_R}^2} \right) \quad (5.2)$$

where

$$A_{LR}^e = \left(\frac{g_{Z_L e_L e_L}^2 - g_{Z_L e_R e_R}^2}{g_{Z_L e_L e_L}^2 + g_{Z_L e_R e_R}^2} \right) \quad (5.3)$$

The currently measured value of $\delta A_{FB}^b = A_{FB}^b|_{\text{exp}} - A_{FB}^b|_{\text{SM}}$ is given by,

$$\delta A_{FB}^b = -0.0038 \pm 0.0016, \quad (5.4)$$

and hence A_{FB}^b exhibits a $\sim 2.3 \sigma$ anomalous departure with respect to the SM prediction [54].

In our model the values of $\delta g_{Z_L b_L b_L}$ and $\delta g_{Z_L b_R b_R}$ are induced by the $Z_L Z_{L,R}^n$ mixing, in turn induced by the electroweak breaking, followed by the corresponding coupling $g_{Z_L b_L b_L}$ or $g_{Z_R b_R b_R}$ ⁵, and by one-loop radiative corrections induced by the operators in Eq. (4.4). An analysis similar to that done in Sec. 4.1 yields the expressions

$$\delta g_{Z_L b_R b_R} = \sum_n \left(\frac{g_R v G_3^n}{2m_n} \right)^2 \left\{ \frac{r_h(\alpha)}{\cos^2 \theta_R} \left[\sin^2 \theta_\Sigma \left(1 - \frac{2}{3} \sin^2 \theta_R \right) - \frac{1}{2} \cos^2 \theta_R \right] \right. \\ \left. + \frac{3h_t^2}{4\pi^2} \log \frac{m_1}{m_t} \left[\frac{2}{9} \sin^2 \theta_R + \frac{1}{\cos^2 \theta_R} \left(\frac{1}{2} - \frac{1}{3} \sin^2 \theta_R \right) \left(\frac{1}{2} - \frac{2}{3} \sin^2 \theta_R \right) \right] \right\} \quad (5.5)$$

and

$$\delta g_{Z_L b_L b_L} = \sum_n \left(\frac{g_R v G_3^n}{2m_n} \right)^2 r_f(c_{b_L}) \sin^2 \theta_R \left\{ r_h(\alpha) \left[\frac{1}{2 \sin^2 \theta_L} - \frac{1}{2} + \frac{\sin^2 \theta_\Sigma}{3 \cos^2 \theta_R} \right] \right. \\ \left. + \frac{3h_t^2}{4\pi^2} \log \frac{m_1}{m_t} \left[-\frac{1}{9} + \frac{1}{6 \cos^2 \theta_R} \left(\frac{1}{2} - \frac{2}{3} \sin^2 \theta_R \right) \right] \right\} \quad (5.6)$$

where, again, the first lines in Eqs. (5.5) and (5.6) are the contributions from the gauge

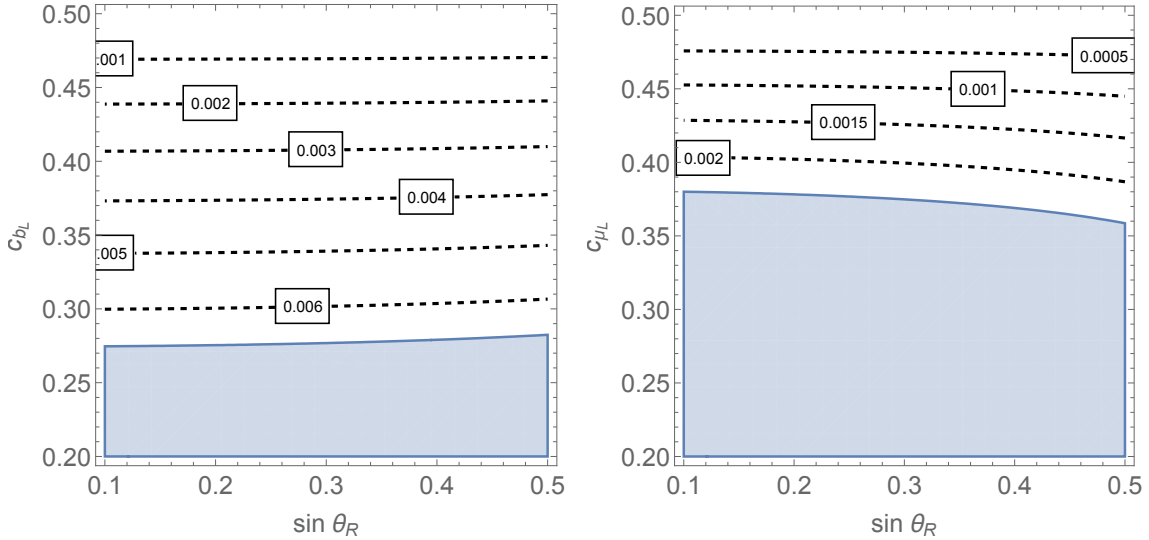


Figure 8: *Left panel: Contour lines of $\delta g_{Z_L b_L b_L}$ in the plane $(\sin \theta_R, c_{b_L})$ where we have fixed $\sin \theta_\Sigma = 0.72$. The white region is allowed by electroweak precision data at the 95% CL. Right panel: The same for $\delta g_{Z_L \mu_L \mu_L}$.*

⁵A related analysis of the bottom forward-backward asymmetry in models with custodial symmetry in warped extra dimensions has been performed in Ref. [55]

bosons KK modes through mixing effects, and the second lines come from the contribution of the radiative corrections induced by the operators

$$\mathcal{O}_{b_{R,L}t_R} = (\bar{b}_{R,L}\gamma^\mu b_{R,L})(\bar{t}_R\gamma_\mu t_R) .$$

Finally, the modification of the left-handed and right-handed bottom couplings to the Z gauge boson induce a modification of A_{FB}^b which, at linear order in $\delta g_{Zb_{L,R}b_{L,R}}$ is given by

$$\delta A_{FB}^b = -0.183 \delta g_{Z_L b_R b_R} - 0.033 \delta g_{Z_L b_L b_L} . \quad (5.7)$$

The shift $\delta g_{Z_L b_L b_L}$ is constrained by electroweak precision data, to be [40]

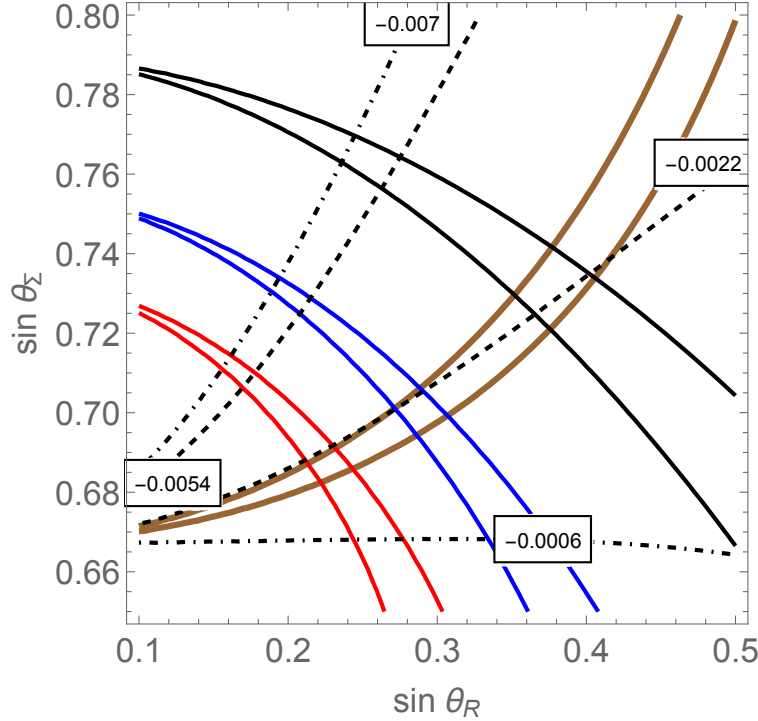


Figure 9: The region between the solid lines is allowed by $\delta g_{Z_L \tau_R \tau_R}$ (brown lines) and by T for $m_1 = 3$ TeV and $\tan \beta = 1$ (black lines) $\tan \beta = 3$ (blue lines) and $\tan \beta = 5$ (red lines). Region between dashed (dot-dashed) lines encompasses the 1σ (2σ) interval for the anomaly in A_{FB}^b .

$$\delta g_{Z_L b_L b_L} = (3.3 \pm 1.7) \times 10^{-3}, \quad (5.8)$$

The region (5.8) constrains the available values of c_{b_L} , as shown in the left panel of Fig. 8, where we have fixed $\sin \theta_\Sigma = 0.72$ and where the shaded area is excluded at the 95% CL.

After fixing the condition to fit $R_{D^{(*)}}$, and using e.g. the value $c_{b_L} = 0.35$, for which $\delta g_{Z_L b_L b_L} \simeq 4.7 \times 10^{-3}$, we find that the 1σ (2σ) experimental value (5.4) is obtained

between the dashed (dot-dashed) lines in Fig. 9, implying that the anomalous value of A_{FB}^b remains consistent with the explanation of the $R_{D^{(*)}}$ anomaly, and the rest of electroweak and LHC constraints, for the parameter region near $\tan \beta = 2 \pm 1$, $\sin \theta_R \simeq 0.32 \pm 0.08$ and $\sin \theta_\Sigma \simeq 0.72 \pm 0.02$. Observe, however, that $\tan \beta$ close to one demands large values of the top-quark Yukawa coupling. As it is clear from Fig. 9, for somewhat larger values of $\tan \beta$ the corrections to the right-handed bottom coupling allow to reduce the current 2.3σ anomaly on A_{FB}^b into a value that is about 1σ away from the central experimental value.

Observe that this custodial symmetry model differs from the results obtained in an abelian gauge symmetry extension of the SM, where an explanation of the forward-backward asymmetry demands the extra gauge bosons to be light, with masses below about 150 GeV, in order to induce small corrections to the T parameter [56].

5.2 The processes $B \rightarrow K \nu \nu$ and $B^+ \rightarrow K^+ \tau^+ \tau^-$

The $R_{D^{(*)}}$ anomaly can in principle induce a large production in the process $B \rightarrow K \bar{\nu} \nu$, i.e. $b \rightarrow s \bar{\nu} \nu$, mainly induced by the RH neutral current Lagrangian ⁶

$$\mathcal{L} = \frac{g_R}{\cos \theta_R} \sum_{n=1}^{\infty} \left\{ (V_{d_R}^\dagger)_{23} g_{Z_R d_R d_R} G_3^n (\bar{s}_R \not{Z}_R^n b_R) + g_{Z_R \nu_R \nu_R} G_3^n (\bar{\nu}_R \not{Z}_R^n \nu_R) \right\} \quad (5.9)$$

where the couplings of Z_R to RH quarks and leptons are given in Eq. (2.21). After integrating out the KK modes we get the effective Lagrangian

$$\begin{aligned} \mathcal{L}_{eff}^{\nu\nu} &= -g_{Z_R d_R d_R} g_{Z_R \nu_R \nu_R} \frac{1}{2 \cos^2 \theta_R} (V_{d_R}^\dagger)_{23} \sum_n \left(\frac{g_R G_3^n}{m_n} \right)^2 (\bar{s}_R \gamma^\mu b_R) (\bar{\nu}_R \gamma_\mu (1 + \gamma_5) \nu) \\ &\equiv -\frac{4G_F}{\sqrt{2}} V_{tb} V_{ts}^* \frac{\alpha_{EM}}{4\pi} C_{\nu\nu} (\bar{s}_R \gamma^\mu b_R) (\bar{\nu}_R \gamma_\mu (1 + \gamma_5) \nu) \end{aligned} \quad (5.10)$$

where we are normalizing $\mathcal{B}(B \rightarrow K \nu_R \nu_R)$ to the SM value of $\sum_\ell \mathcal{B}(B \rightarrow K \nu_\ell \nu_\ell)$, and the Wilson coefficient $C_{\nu\nu}$ is given by

$$C_{\nu\nu} = \frac{1}{2 \cos^2 \theta_R} \left(\frac{1}{2} - \frac{1}{3} \sin^2 \theta_R \right) \frac{4\pi}{\alpha_{EM}} (V_{d_R}^\dagger)_{23} \frac{1}{V_{cb}} \sum_n \left(\frac{g_R G_3^n}{2m_n} \right)^2 \quad (5.11)$$

and where we have used that in the Wolfenstein parametrization $V_{cb} = -V_{ts} = A\lambda^2$, and $V_{tb} = 1$.

Now we can write the ratio

$$R_K^{\nu\nu} = \frac{\mathcal{B}(B \rightarrow K \nu \nu)}{\mathcal{B}(B \rightarrow K \nu \nu)_{SM}} = 1 + \frac{1}{3} \frac{|C_{\nu\nu}|^2}{|C_{\nu\nu}^{SM}|^2} \simeq 1 + 0.008 |C_{\nu\nu}|^2, \quad (5.12)$$

⁶Notice that $g_{Z_L \nu_R \nu_R} = g_{A \nu_R \nu_R} = 0$ and hence no Z_L^n or A^n mediated processes occur.

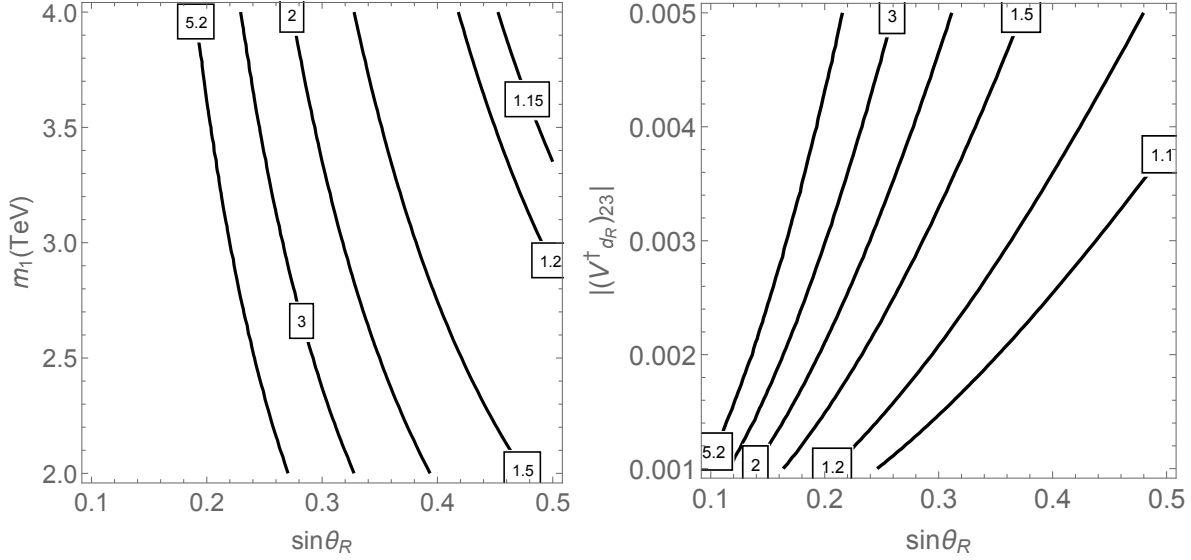


Figure 10: *Left panel: Contour lines of constant $R_K^{\nu\nu}$ where we have used the upper bound on $(V_{d_R}^\dagger)_{23} = 0.005$ obtained by the condition given in Eq. (4.33). Right panel: Contour lines of $R_K^{\nu\nu}$ for $m_1 = 3$ TeV.*

where we have used the SM prediction $C_{\nu\nu}^{SM} \simeq -6.4$ [57]. Using the experimental bound $R_K^{\nu\nu} < 5.2$ at the 95% CL [14], one finds the bound $|C_{\nu\nu}| \lesssim 23$. However, after imposing the constraints coming from the flavor condition (4.33) on the matrix element $(V_{d_R}^\dagger)_{23}$, one easily obtains values that are well below the experimental bound, particularly for values of $\sin \theta_R > 0.2$. This is shown in the left panel of Fig. 10, where we plot contours of constant $R_K^{\nu\nu}$ in the plane $(\sin \theta_R, m_1)$ after using the bound for $(V_{d_R}^\dagger)_{23}$ in Eq. (4.33). Lower values of $R_K^{\nu\nu}$ may be obtained for smaller values of $\sin \theta_R$ by using the freedom on the value of $(V_{d_R}^\dagger)_{23}$, as shown in the right panel of Fig. 10, where we plot $R_K^{\nu\nu}$ in the plane $(\sin \theta_R, (V_{d_R}^\dagger)_{23})$ after fixing $m_1 = 3$ TeV.

This model predicts a strong $\tau\tau$ production in the observable

$$R_K^\tau = \frac{\mathcal{B}(B^+ \rightarrow K^+ \tau \tau)}{\mathcal{B}(B^+ \rightarrow K^+ \tau \tau)_{SM}} \quad (5.13)$$

In our model this observable is dominated by the Wilson coefficient C_{RR}^τ such that

$$R_K^\tau \simeq 1 + \left| \frac{C_{RR}^\tau}{C_{LL}^{SM}} \right|^2 \quad (5.14)$$

where

$$C_{RR}^\tau = -\frac{8\pi}{\alpha_{EM}} \sum_n \left(\frac{g_R v G_3^n}{2m_n} \right)^2 \frac{(V_{d_R}^\dagger)_{23}}{V_{ts}^*} \left[\frac{1}{3} \sin^2 \theta_R + \frac{1}{\cos^2 \theta_R} \left(\frac{1}{2} - \frac{1}{3} \sin^2 \theta_R \right) \left(\frac{1}{2} - \sin^2 \theta_R \right) \right] \quad (5.15)$$

Contour lines of constant R_K^τ are presented in Fig. 11 for $m_1 = 3$ TeV. The results are

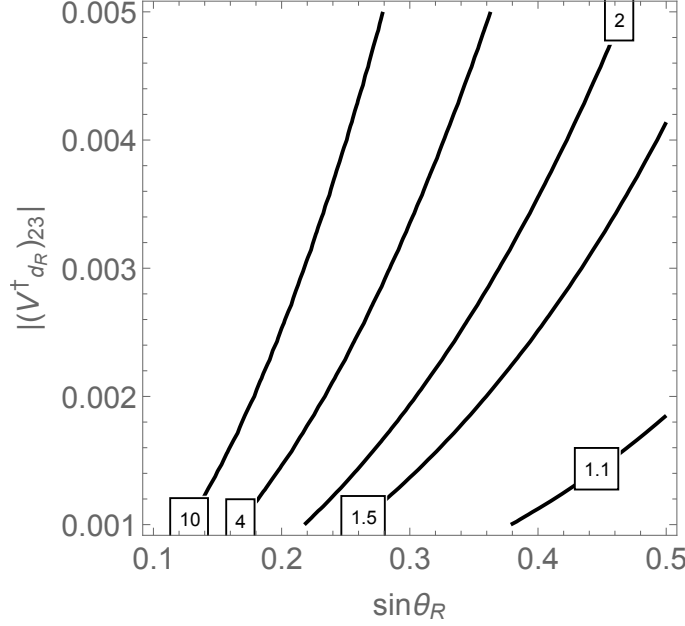


Figure 11: *Contour lines of R_K^τ in the plane $[\sin \theta_R, |(V_{d_R}^\dagger)_{23}|]$, for values of $(V_{d_R}^\dagger)_{23}$ consistent with the flavor constraints.*

widely consistent with present experimental bounds from the BaBar Collaboration [58] which yield the 90% CL upper bound, $R_K^\tau < 10^4$.

5.3 $R_{K^{(*)}}$

One of the general applications of our theory is that it generically predicts a value of $R_{K^{(*)}}$

$$R_{K^{(*)}} = \frac{\text{BR}(B \rightarrow K^{(*)} \mu^+ \mu^-)}{\text{BR}(B \rightarrow K^{(*)} e^+ e^-)}, \quad (5.16)$$

which can easily differ from its SM prediction [59, 60]. The general effective operator Lagangian is written as

$$\mathcal{L}_{eff} = \frac{4G_F}{\sqrt{2}} \frac{\alpha_{EM}}{4\pi} V_{ts}^* V_{tb} \sum_i C_i \mathcal{O}_i. \quad (5.17)$$

We will find it convenient to work in the chiral basis for the operators \mathcal{O}_i such that operators

$$\mathcal{O}_{\chi\chi'} = (\bar{s}_\chi \gamma^\mu b_\chi) (\bar{\ell}_{\chi'} \gamma_\mu \ell_{\chi'}) \quad (5.18)$$

with chiralities $\chi, \chi' = \{L, R\}$, have Wilson coefficients defined as $C_{\chi\chi'}^\ell \equiv C_{\chi\chi'}^{SM} + \Delta C_{\chi\chi'}^\ell$ ⁷. The SM predictions are given by

$$C_{LL}^{SM} \simeq 8.4, \quad C_{RL}^{SM} \simeq C_{LR}^{SM} \simeq C_{RR}^{SM} \simeq 0 \quad (5.19)$$

while $\Delta C_{\chi\chi'}^\ell$ are the contributions to the Wilson coefficients coming from New Physics.

The prediction of $R_{K^{(*)}}$ is given by

$$R_{K^{(*)}} = \frac{|C_{LL}^\mu + C_{LR}^\mu \pm C_{RL}^\mu \pm C_{RR}^\mu|^2 + |C_{LR}^\mu - C_{LL}^\mu \pm C_{RR}^\mu \mp C_{RL}^\mu|^2}{|C_{LL}^e + C_{LR}^e \pm C_{RL}^e \pm C_{RR}^e|^2 + |C_{LR}^e - C_{LL}^e \pm C_{RR}^e \mp C_{RL}^e|^2} \quad (5.20)$$

where the upper signs correspond to R_K and the lower signs to R_{K^*} and we have assumed that the polarization of the K^* is close to $p = 1$, what is a good approximation in the relevant q^2 region associated with the R_{K^*} measurement [62]. The above equation, Eq. (5.20), shows the well known correlation (anti-correlation) of the corrections to R_K and R_{K^*} associated to the left- (right-) handed currents. Therefore, considering the fact that both R_K and R_{K^*} are suppressed with respect to the SM values, this leads to a preference of new physics effects involving left-handed currents.

The experimental value of $R_{K^{(*)}}$ departs from the SM prediction $R_{K^{(*)}} \simeq 1$ [63] by around 2.5σ . Moreover global fits [64–70] to a number of observables, including the branching ratios for $B \rightarrow K^* \ell \ell$, $B_s \rightarrow \phi \mu \mu$, and $B_s \rightarrow \mu \mu$, favor a solution where $\Delta C_{LL}^\mu < 0$ while $\Delta C_{RL}^\mu \simeq \Delta C_{LR}^\mu \simeq \Delta C_{RR}^\mu \simeq 0$, and $\Delta C_{\chi, \chi'}^e \simeq 0$ for $\chi, \chi' = \{L, R\}$.

In fact, in our model, for

$$c_{eL,R} \gtrsim 1/2, \quad c_{\mu R} \gtrsim 1/2 \quad (5.21)$$

it turns out that $C_{\chi\chi'}^e \simeq C_{\chi\chi'}^{SM}$ and $\Delta C_{LR}^\mu \simeq \Delta C_{RR}^\mu \simeq 0$ ⁸. On the other hand the prediction for ΔC_{LL}^μ is given by

$$\Delta C_{LL}^\mu = -\frac{8\pi}{\alpha_{EM}} \sum_n \left(\frac{g_R v G_3^n}{2m_n} \right)^2 r_f(c_{bL}) r_f(c_{\mu L}) \cdot \left[\sin^2 \theta_R \left[\left(\frac{1}{2 \sin^2 \theta_L} - \frac{1}{3} \right) \left(\frac{1}{2} - \sin^2 \theta_L \right) + \frac{1}{3} \cos^2 \theta_L - \frac{1}{12} \frac{\sin^2 \theta_R}{\cos^2 \theta_R} \right] \right] \quad (5.22)$$

where the first, second and third terms inside the square bracket comes from the contribution of the Z_L^n , A^n and Z_R^n KK modes, respectively, and we are assuming [71] that

⁷The relation with the usual non-chiral basis, $C_{9,10}^{(\prime)}$, [61] is given by: $C_{LL} = C_9 - C_{10}$, $C_{LR} = C_9 + C_{10}$, $C_{RL} = C'_9 - C'_{10}$ and $C_{RR} = C'_9 + C'_{10}$.

⁸Or, in the usual basis language, $\Delta C_9^\mu = -\Delta C_{10}^\mu$ and $\Delta C_{9,10}^{\prime\mu} \simeq 0$.

$V_{u_L} \simeq 1$ and $V_{d_L} \simeq V$, the CKM matrix. Similarly, the prediction for ΔC_{RL}^μ is given by

$$\Delta C_{RL}^\mu = -\frac{8\pi}{\alpha_{EM}} \sum_n \left(\frac{g_{R\nu} G_3^n}{2m_n} \right)^2 r_f(c_{\mu_L}) \left[(V_{d_R}^\dagger)_{23}/V_{ts}^* \right] \cdot \sin^2 \theta_R \left[\frac{1}{3} \left(-\frac{1}{2} + \sin^2 \theta_L \right) + \frac{1}{3} \cos^2 \theta_L + \frac{1}{2 \cos^2 \theta_R} \left(-\frac{1}{2} + \frac{1}{3} \sin^2 \theta_R \right) \right]. \quad (5.23)$$

Observe that the combined contribution to ΔC_{LL}^μ from the Z_L^n and A^n KK modes is considerably larger than the one from the Z_R^n KK modes. Recent global fits to experimental

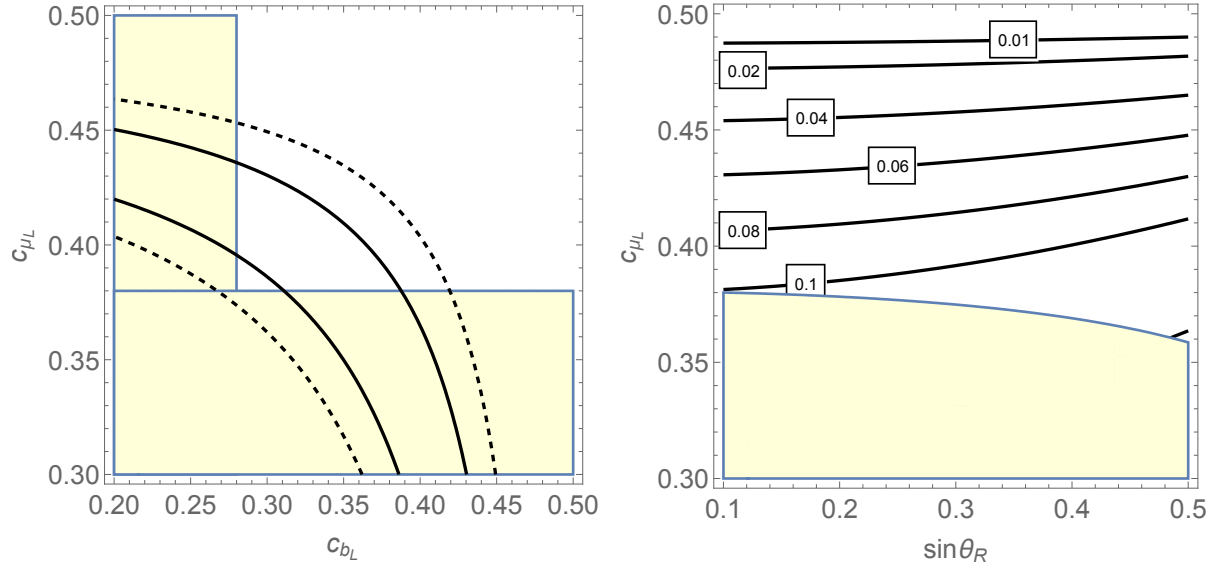


Figure 12: *Left panel: Contour lines of constant ΔC_{LL}^μ in the plane (c_{b_L}, c_{μ_L}) using $V_{d_L} \simeq V$, at 1 σ (solid lines) and 2 σ (dashed lines) level as defined in Eq. (5.24). The value of $\sin \theta_R = 0.35$ has been fixed. Right panel: Contour lines of constant ΔC_{RL}^μ in the plane $(\sin \theta_R, c_{\mu_L})$ after selecting the upper bound on $|(V_{d_R}^\dagger)_{23}| \simeq 0.005$ obtained in Eq. (4.33). In both panels the shaded yellow area corresponds to the excluded area obtained in Fig. 8.*

data [68] yield the 1 σ (2 σ) prediction

$$\Delta C_{LL}^\mu \subset [-1.66, -1.04]_{1\sigma}, [-1.98, -0.76]_{2\sigma} \quad (5.24)$$

which constitutes a $\sim 4.8 \sigma$ deviation with respect to the SM prediction. On the other hand C_{RL}^μ has to be small and in fact the global fit yields [68]

$$\Delta C_{RL}^\mu \subset [-0.04, 0.36]_{1\sigma}, [-0.24, 0.56]_{2\sigma} \quad (5.25)$$

which only depart $\sim 0.8 \sigma$ from the SM prediction.

The left panel of Fig. 12 shows the 1σ (solid lines) and 2σ contours of ΔC_{LL}^μ in the plane (c_{b_L}, c_{μ_L}) , where we have fixed $\sin\theta_R = 0.35$. The values of c_{b_L} and c_{μ_L} are mainly constrained from $\delta g_{Z_L b_L b_L}$, as given in Eq. (5.6), and plotted in the left panel of Fig. 8, and from $\delta g_{Z_L \mu_L \mu_L}$ as given by

$$\begin{aligned} \delta g_{Z_L \mu_L \mu_L} = & \sum_n \left(\frac{g_R v G_3^n}{2m_n} \right)^2 r_f(c_{\mu_L}) \sin^2 \theta_R \left\{ r_h(\alpha) \left[\frac{1}{2 \sin^2 \theta_L} - \frac{1}{2} - \frac{\sin^2 \theta_\Sigma}{\cos^2 \theta_R} \right] \right. \\ & \left. + \frac{1}{12 \cos^2 \theta_R} \frac{3h_t^2}{4\pi^2} \log \frac{m_1}{m_t} \right\}, \end{aligned} \quad (5.26)$$

where, again, the first line in Eq. (5.26) denote the contributions from the gauge bosons KK modes through the mixing and the second line denote those from the radiative corrections induced by the operators

$$\mathcal{O}_{\mu_L t_R} = (\bar{\mu}_L \gamma^\mu \mu_L)(\bar{t}_R \gamma_\mu t_R).$$

The prediction for $\delta g_{Z_L \mu_L \mu_L}$ is plotted in the right panel of Fig. 8, where we also have fixed $\sin\theta_\Sigma = 0.72$, and where the white region is allowed at the 95% CL given the fitted value to experimental data [40]

$$\delta g_{Z_L \mu_L \mu_L} = (0.1 \pm 1.2) \times 10^{-3}. \quad (5.27)$$

Moreover, from Fig. 8 at 95% CL, $c_{b_L} \gtrsim 0.28$ and $c_{\mu_L} \gtrsim 0.38$, independently on the value of $\sin\theta_R$. The forbidden regions in Fig. 12 are represented by shaded light-yellow areas.

The prediction for C_{RL}^μ is shown in the right panel of Fig. 12 in the plane $(\sin\theta_R, c_{\mu_L})$ where we are already using the upper bound on $(V_{d_R}^\dagger)_{23}$ from flavor observables, while the shaded region is excluded by $\delta g_{Z_L \mu_L \mu_L}$. We see that the values of ΔC_{RL}^μ in the region defined by Eq. (5.20) are always $\lesssim \mathcal{O}(0.1)$ and hence in accordance with the global fits, Eq. (5.25).

6 Conclusions

The experimental measurements of $R_{D^{(*)}}$ show significant deviations from the SM values, a surprising result due to the tree-level nature of this process in the SM. Possible resolutions of this anomaly face significant constraints from the excellent agreement of flavor physics observables with the values predicted within the SM. In this work, we have presented an explicit realization of the solution to the $R_{D^{(*)}}$ anomaly based on the contribution of right-handed currents of quarks and leptons to this process. The model is based on the embedding of the SM in warped space, with a bulk gauge symmetry $SU(2)_L \otimes SU(2)_R \otimes$

$U(1)_{B-L}$, with third-generation right-handed quarks and leptons localized on the infrared-brane, ensuring a large coupling of these modes to the charged gauge boson W_R^n KK-modes.

The right-handed $SU(2)_R$ gauge boson KK-modes provide the necessary contribution to $R_{D^{(*)}}$, due to relevant mixing parameters in the right-handed up-quark sector. This may be done without inducing large contributions to the B -meson invisible decays, or the B -meson mixings, since these observables strongly depend on the down-quark right handed mixing angles, which do not affect $R_{D^{(*)}}$ in any significant way within this framework. The mass of the lightest KK-mode tends to be of about a few TeV, and it is in natural agreement with current LHC constraints.

An important assumption within this model is that there is no mixing in the lepton sector. This can be ensured with appropriate symmetries, that must be (softly) broken in order to allow the proper neutrino mixing. We have presented a scenario, based on symmetries and a double seesaw mechanism, that allows for a proper description of the lepton sector of the model. The origin of the new parameters in the lepton sector remains, however, as one of the most challenging aspects of these (and many) scenarios. Aside of this question, beyond providing a resolution to the $R_{D^{(*)}}$ anomaly, this model also provides a solution of the hierarchy problem, has an explicit custodial symmetry that implies small corrections to the precision electroweak observables, and allows a solution to the $R_{K^{(*)}}$ anomalies mainly via the contribution of the $SU(2)_L$ KK modes. Moreover, the proposed model naturally predicts an anomalous value of the forward-backward asymmetry A_{FB}^b , as implied by LEP data, driven by the $Z\bar{b}_R b_R$ coupling.

ACKNOWLEDGMENTS

This manuscript has been authored by Fermi Research Alliance, LLC under Contract No. DE-AC02-07CH11359 with the U.S. Department of Energy, Office of Science, Office of High Energy Physics. The United States Government retains and the publisher, by accepting the article for publication, acknowledges that the United States Government retains a non-exclusive, paid-up, irrevocable, world-wide license to publish or reproduce the published form of this manuscript, or allow others to do so, for United States Government purposes. Work at University of Chicago is supported in part by U.S. Department of Energy grant number DE-FG02-13ER41958. Work at ANL is supported in part by the U.S. Department of Energy under Contract No. DE-AC02-06CH11357. The work of E.M. is supported by the Spanish MINEICO and European FEDER funds grant number FIS2017-85053-C2-1-P, and by the Junta de Andalucía grant number FQM-225. The research of E.M. is also supported by the Ramón y Cajal Program of the Spanish MINEICO. The work of M.Q. is partly supported by Spanish MINEICO under Grant CICYT-FEDER-FPA2014-55613-P and FPA2017-88915-P, and by the Severo Ochoa Excellence Program of MINEICO under Grant SEV-2016-0588. M.Q. would like to thank the Argonne Na-

tional Laboratory and the Fermi National Accelerator Laboratory, where part of this work has been done, for hospitality and the Argonne National Laboratory for financial support. We would like to thank Antonio Delgado, Admiri Greljo, Da Liu, J. Liu, E. Stamou, N.R. Shah, David Shih and Jure Zupan for useful discussions, and specially X. Wang, for her help in computing the LHC KK gauge boson cross sections. E.M., M.Q. and C.W. would like to thank the Mainz Institute for Theoretical Physics, and M.C. and C.W. the Aspen Center for Physics, which is supported by National Science Foundation grant PHY-1607611, for the kind hospitality during the completion of this work.

A The KK-modes

The KK-modes of the gauge bosons can be obtained by solving the equation of motion

$$m_A^2 f_A + \left(e^{-2y} \dot{f}_A \right)' = 0. \quad (\text{A.1})$$

where we are using the notation $\dot{f} \equiv df/dy$. The $(+, +)$ boundary conditions lead to the following wavefunction

$$f_A^{(+,+)}(y) = C_0^{(+,+)} e^{ky} \left[J_1(e^{ky-ky_1} \hat{m}) + C_1^{(+,+)} Y_1(e^{ky-ky_1} \hat{m}) \right], \quad (\text{A.2})$$

where

$$C_1^{(+,+)} = -\frac{J_0(e^{-ky_1} \hat{m})}{Y_0(e^{-ky_1} \hat{m})} \quad (\text{A.3})$$

guarantees the Neumann boundary condition in the UV brane, and J_α and Y_α correspond to the Bessel functions of the first and second kind respectively. We have defined here $\hat{m} \equiv m/\rho$ with $\rho = e^{-ky_1} k$.

By the same way, the boundary conditions $(-, +)$ lead to

$$f_A^{(-,+)}(y) = C_0^{(-,+)} e^{ky} \left[J_1(e^{ky-ky_1} \hat{m}) + C_1^{(-,+)} Y_1(e^{ky-ky_1} \hat{m}) \right], \quad (\text{A.4})$$

where

$$C_1^{(-,+)} = -\frac{J_1(e^{-ky_1} \hat{m})}{Y_1(e^{-ky_1} \hat{m})} \quad (\text{A.5})$$

guarantees the Dirichlet boundary condition in the UV brane. In these expressions $C_0^{(+,+)}$ and $C_0^{(-,+)}$ are arbitrary constants. Notice that a constant $f_A(y)$ fulfills the $(+, +)$ boundary conditions, and from Eq. (A.1) one finds that this corresponds to a zero mode. The $(-, +)$ boundary conditions, however, do not lead to zero modes.

In the limit of large ky_1 , the Neumann boundary conditions in the IR brane lead to the following equations for the eigenvalues

$$0 = J_0(\hat{m}_{++}) + \frac{\pi}{2} Y_0(\hat{m}_{++}) \frac{1}{ky_1} + \mathcal{O}(1/k^2 y_1^2), \quad (\text{A.6})$$

$$0 = J_0(\hat{m}_{-+}) + \frac{\pi}{4} \hat{m}_{-+}^2 Y_0(\hat{m}_{-+}) e^{-2ky_1} + \mathcal{O}(e^{-4ky_1}), \quad (\text{A.7})$$

for $(+, +)$ and $(-, +)$ boundary conditions respectively. Taking into account the expansion of the Bessel function $J_0(\hat{m} + \delta\hat{m}) = J_0(\hat{m}) - J_1(\hat{m})\delta\hat{m} + \mathcal{O}(\delta\hat{m}^2)$, one finds the following eigenvalues

$$\hat{m}_{++}^{(n)} = \hat{m}_0^{(n)} + \frac{\pi}{2} \frac{Y_0(\hat{m}_0^{(n)})}{J_1(\hat{m}_0^{(n)})} \frac{1}{ky_1} + \mathcal{O}(1/k^2 y_1^2), \quad (\text{A.8})$$

$$\hat{m}_{-+}^{(n)} = \hat{m}_0^{(n)} + \frac{\pi}{4} \hat{m}_0^{(n)2} \frac{Y_0(\hat{m}_0^{(n)})}{J_1(\hat{m}_0^{(n)})} e^{-2ky_1} + \mathcal{O}(e^{-4ky_1}), \quad (\text{A.9})$$

where $\hat{m}_0^{(n)}$ is the n -th zero of the $J_0(\hat{m})$ function, in particular:

$$\hat{m}_0^{(n)} = \{2.405, 5.520, 8.654, 11.792, 14.931, \dots\}.$$

The second term in the right-hand side of Eq. (A.9) leads to corrections of $\mathcal{O}(10^{-28}) - \mathcal{O}(10^{-30})$ for the five lightest eigenvalues when $ky_1 = 35$, so that this correction can be considered negligible. The correction in Eq. (A.8) is ≈ 0.045 , so the difference between the eigenvalues is then

$$\hat{m}_{++}^{(n)} - \hat{m}_{-+}^{(n)} = \frac{\pi}{2} \frac{Y_0(\hat{m}_0^{(n)})}{J_1(\hat{m}_0^{(n)})} \frac{1}{ky_1} + \mathcal{O}(1/k^2 y_1^2) \quad (\text{A.10})$$

of order 0.045 for all the modes. This difference will be neglected throughout this paper.

Let us now compute the value of the coupling $f_{W_R}^n(ky_1) = f_A^{(-,+),n}(ky_1)$, where we are normalizing the wave functions such that, Eq. (2.18),

$$\int_0^{y_1} dy f_A^2(y) = y_1. \quad (\text{A.11})$$

The function $f_A(y)$ grows with y , so that this integral is dominated by the regime close to $y \simeq y_1$. In this regime the dominant contribution to the wave function is the term $\sim e^{ky} J_1(e^{ky-k y_1} \hat{m})$ in Eqs. (A.2) and (A.4), i.e.

$$f_A(y) \simeq C_0 e^{ky} J_1(e^{ky-k y_1} \hat{m}). \quad (\text{A.12})$$

If we focus on the $(-+)$ solution, then one has

$$\begin{aligned}
y_1 &\simeq (C_0^{(-,+)})^2 \int_0^{y_1} dy e^{2ky} [J_1(e^{ky-ky_1}\hat{m})]^2 \\
&\simeq (C_0^{(-,+)})^2 \int_0^{y_1} dy e^{2ky} \left([J_1(e^{ky-ky_1}\hat{m})]^2 + J_1(e^{ky-ky_1}\hat{m}) \frac{1}{k} \frac{d}{dy} J_1(e^{ky-ky_1}\hat{m}) \right) \\
&= \frac{1}{2k} (C_0^{(-,+)})^2 \int_0^{y_1} dy \frac{d}{dy} \left[e^{2ky} [J_1(e^{ky-ky_1}\hat{m})]^2 \right] \\
&\simeq \frac{1}{2k} (C_0^{(-,+)})^2 e^{2ky_1} [J_1(\hat{m})]^2.
\end{aligned} \tag{A.13}$$

In the second equality we have added a term whose integral is vanishing when \hat{m} is an eigenvalue of $J_0(\hat{m})$. To see this, let us note that

$$e^{2ky} J_1(e^{ky-ky_1}\hat{m}) \frac{d}{dy} J_1(e^{ky-ky_1}\hat{m}) = \frac{d}{dy} \left[\frac{1}{2} e^{2ky} J_0(e^{ky-ky_1}\hat{m}) J_2(e^{ky-ky_1}\hat{m}) \right]. \tag{A.14}$$

This implies that after integrating this term in $\int_0^{y_1} dy$, the result is $\propto J_0(\hat{m})$, which is vanishing⁹. From Eqs. (A.12) and (A.13) one finally finds

$$|f_A^{(-+),n}(y_1)| \simeq \sqrt{2ky_1}. \tag{A.15}$$

This result is valid for any eigenvalue, in the approximation where we are neglecting corrections of $\mathcal{O}(e^{-2ky_1})$ for the lightest eigenvalues. The wave functions with boundary conditions $(++)$ have some small deviations with respect to Eq. (A.15) but we also find $|f_A^{(++) ,n}(y_1)| \simeq \sqrt{2ky_1}$ for the non-vanishing modes. Therefore in this paper we will use the approximation where

$$|f_A^{(++) ,n}(y_1)| \simeq |f_A^{(-+),n}(y_1)| \simeq \sqrt{2ky_1}. \tag{A.16}$$

References

- [1] ATLAS collaboration, G. Aad et al., *Observation of a new particle in the search for the Standard Model Higgs boson with the ATLAS detector at the LHC*, *Phys. Lett. B* **716** (2012) 1–29, [[1207.7214](#)].
- [2] CMS collaboration, S. Chatrchyan et al., *Observation of a new boson at a mass of 125 GeV with the CMS experiment at the LHC*, *Phys. Lett. B* **716** (2012) 30–61, [[1207.7235](#)].

⁹We are neglecting terms as $J_\alpha(e^{-ky_1}\hat{m})$, since we consider large ky_1 values.

- [3] PARTICLE DATA GROUP collaboration, C. Patrignani et al., *Review of Particle Physics*, *Chin. Phys.* **C40** (2016) 100001.
- [4] BABAR collaboration, J. P. Lees et al., *Evidence for an excess of $\bar{B} \rightarrow D^{(*)}\tau^-\bar{\nu}_\tau$ decays*, *Phys. Rev. Lett.* **109** (2012) 101802, [[1205.5442](#)].
- [5] BABAR collaboration, J. P. Lees et al., *Measurement of an Excess of $\bar{B} \rightarrow D^{(*)}\tau^-\bar{\nu}_\tau$ Decays and Implications for Charged Higgs Bosons*, *Phys. Rev.* **D88** (2013) 072012, [[1303.0571](#)].
- [6] BELLE collaboration, M. Huschle et al., *Measurement of the branching ratio of $\bar{B} \rightarrow D^{(*)}\tau^-\bar{\nu}_\tau$ relative to $\bar{B} \rightarrow D^{(*)}\ell^-\bar{\nu}_\ell$ decays with hadronic tagging at Belle*, *Phys. Rev.* **D92** (2015) 072014, [[1507.03233](#)].
- [7] BELLE collaboration, Y. Sato et al., *Measurement of the branching ratio of $\bar{B}^0 \rightarrow D^{*+}\tau^-\bar{\nu}_\tau$ relative to $\bar{B}^0 \rightarrow D^{*+}\ell^-\bar{\nu}_\ell$ decays with a semileptonic tagging method*, *Phys. Rev.* **D94** (2016) 072007, [[1607.07923](#)].
- [8] BELLE collaboration, S. Hirose et al., *Measurement of the τ lepton polarization and $R(D^*)$ in the decay $\bar{B} \rightarrow D^*\tau^-\bar{\nu}_\tau$* , *Phys. Rev. Lett.* **118** (2017) 211801, [[1612.00529](#)].
- [9] BELLE collaboration, A. Abdesselam et al., *Measurement of the branching ratio of $\bar{B}^0 \rightarrow D^{*+}\tau^-\bar{\nu}_\tau$ relative to $\bar{B}^0 \rightarrow D^{*+}\ell^-\bar{\nu}_\ell$ decays with a semileptonic tagging method*, in *Proceedings, 51st Rencontres de Moriond on Electroweak Interactions and Unified Theories: La Thuile, Italy, March 12-19, 2016*, 2016. [1603.06711](#).
- [10] A. Abdesselam et al., *Measurement of the τ lepton polarization in the decay $\bar{B} \rightarrow D^*\tau^-\bar{\nu}_\tau$* , [1608.06391](#).
- [11] LHCb collaboration, R. Aaij et al., *Measurement of the ratio of branching fractions $\mathcal{B}(\bar{B}^0 \rightarrow D^{*+}\tau^-\bar{\nu}_\tau)/\mathcal{B}(\bar{B}^0 \rightarrow D^{*+}\mu^-\bar{\nu}_\mu)$* , *Phys. Rev. Lett.* **115** (2015) 111803, [[1506.08614](#)].
- [12] BABAR collaboration, J. P. Lees et al., *Search for $B \rightarrow K^{(*)}\nu\bar{\nu}$ and invisible quarkonium decays*, *Phys. Rev.* **D87** (2013) 112005, [[1303.7465](#)].
- [13] BELLE collaboration, O. Lutz et al., *Search for $B \rightarrow h^{(*)}\nu\bar{\nu}$ with the full Belle $\Upsilon(4S)$ data sample*, *Phys. Rev.* **D87** (2013) 111103, [[1303.3719](#)].
- [14] BELLE collaboration, J. Grygier et al., *Search for $B \rightarrow h\nu\bar{\nu}$ decays with semileptonic tagging at Belle*, *Phys. Rev.* **D96** (2017) 091101, [[1702.03224](#)].
- [15] P. Asadi, M. R. Buckley and D. Shih, *It's all right(-handed neutrinos): a new W' model for the $R_{D^{(*)}}$ anomaly*, [1804.04135](#).

- [16] A. Greljo, D. J. Robinson, B. Shakya and J. Zupan, *$R(D^{(*)})$ from W' and right-handed neutrinos*, [1804.04642](#).
- [17] R. N. Mohapatra and J. C. Pati, *Left-Right Gauge Symmetry and an Isoconjugate Model of CP Violation*, *Phys. Rev.* **D11** (1975) 566–571.
- [18] R. N. Mohapatra and J. C. Pati, *A Natural Left-Right Symmetry*, *Phys. Rev.* **D11** (1975) 2558.
- [19] G. Senjanovic and R. N. Mohapatra, *Exact Left-Right Symmetry and Spontaneous Violation of Parity*, *Phys. Rev.* **D12** (1975) 1502.
- [20] K. Agashe, A. Delgado, M. J. May and R. Sundrum, *$RS1$, custodial isospin and precision tests*, *JHEP* **08** (2003) 050, [[hep-ph/0308036](#)].
- [21] M. Blanke, A. J. Buras, B. Duling, S. Gori and A. Weiler, *$\Delta F=2$ Observables and Fine-Tuning in a Warped Extra Dimension with Custodial Protection*, *JHEP* **03** (2009) 001, [[0809.1073](#)].
- [22] M. Blanke, A. J. Buras, B. Duling, K. Gemmler and S. Gori, *Rare K and B Decays in a Warped Extra Dimension with Custodial Protection*, *JHEP* **03** (2009) 108, [[0812.3803](#)].
- [23] E. Megias, G. Panico, O. Pujolas and M. Quiros, *A Natural origin for the LHCb anomalies*, *JHEP* **09** (2016) 118, [[1608.02362](#)].
- [24] E. Megias, M. Quiros and L. Salas, *Lepton-flavor universality violation in R_K and $R_{D^{(*)}}$ from warped space*, *JHEP* **07** (2017) 102, [[1703.06019](#)].
- [25] E. Megias, M. Quiros and L. Salas, *Lepton-flavor universality limits in warped space*, *Phys. Rev.* **D96** (2017) 075030, [[1707.08014](#)].
- [26] L. Randall and R. Sundrum, *A Large mass hierarchy from a small extra dimension*, *Phys. Rev. Lett.* **83** (1999) 3370–3373, [[hep-ph/9905221](#)].
- [27] W. D. Goldberger and M. B. Wise, *Modulus stabilization with bulk fields*, *Phys. Rev. Lett.* **83** (1999) 4922–4925, [[hep-ph/9907447](#)].
- [28] E. Megias, G. Panico, O. Pujolas and M. Quiros, *A natural extra-dimensional origin for the LHCb anomalies*, in *Proceedings, 52nd Rencontres de Moriond on Electroweak Interactions and Unified Theories: La Thuile, Italy, March 18-25, 2017*, pp. 225–232, 2017. [1705.04822](#).
- [29] S. J. Huber, *Flavor violation and warped geometry*, *Nucl. Phys.* **B666** (2003) 269–288, [[hep-ph/0303183](#)].

- [30] G. Moreau and J. I. Silva-Marcos, *Neutrinos in warped extra dimensions*, *JHEP* **01** (2006) 048, [[hep-ph/0507145](#)].
- [31] C. Csaki, C. Delaunay, C. Grojean and Y. Grossman, *A Model of Lepton Masses from a Warped Extra Dimension*, *JHEP* **10** (2008) 055, [[0806.0356](#)].
- [32] G. Perez and L. Randall, *Natural Neutrino Masses and Mixings from Warped Geometry*, *JHEP* **01** (2009) 077, [[0805.4652](#)].
- [33] G. von Gersdorff, M. Quiros and M. Wiechers, *Neutrino Mixing from Wilson Lines in Warped Space*, *JHEP* **02** (2013) 079, [[1208.4300](#)].
- [34] S. M. Barr, *A Different seesaw formula for neutrino masses*, *Phys. Rev. Lett.* **92** (2004) 101601, [[hep-ph/0309152](#)].
- [35] R. Alonso, B. Grinstein and J. Martin Camalich, *Lifetime of B_c^- Constrains Explanations for Anomalies in $B \rightarrow D^{(*)}\tau\nu$* , *Phys. Rev. Lett.* **118** (2017) 081802, [[1611.06676](#)].
- [36] LHCb collaboration, R. Aaij et al., *Measurement of the ratio of branching fractions $\mathcal{B}(B_c^+ \rightarrow J/\psi\tau^+\nu_\tau)/\mathcal{B}(B_c^+ \rightarrow J/\psi\mu^+\nu_\mu)$* , *Phys. Rev. Lett.* **120** (2018) 121801, [[1711.05623](#)].
- [37] A. Issadykov and M. A. Ivanov, *The decays $B_c \rightarrow J/\psi + \bar{\ell}\nu_\ell$ and $B_c \rightarrow J/\psi + \pi(K)$ in covariant confined quark model*, *Phys. Lett.* **B783** (2018) 178–182, [[1804.00472](#)].
- [38] T. D. Cohen, H. Lamm and R. F. Lebed, *Model-Independent Bounds on $R(J/\psi)$* , [1807.02730](#).
- [39] F. Feruglio, P. Paradisi and A. Pattori, *On the Importance of Electroweak Corrections for B Anomalies*, *JHEP* **09** (2017) 061, [[1705.00929](#)].
- [40] A. Falkowski, M. Gonzalez-Alonso and K. Mimouni, *Compilation of low-energy constraints on 4-fermion operators in the SMEFT*, [1706.03783](#).
- [41] M. Carena, A. Delgado, E. Ponton, T. M. P. Tait and C. E. M. Wagner, *Warped fermions and precision tests*, *Phys. Rev.* **D71** (2005) 015010, [[hep-ph/0410344](#)].
- [42] M. Carena, E. Ponton, J. Santiago and C. E. M. Wagner, *Light Kaluza Klein States in Randall-Sundrum Models with Custodial $SU(2)$* , *Nucl. Phys.* **B759** (2006) 202–227, [[hep-ph/0607106](#)].
- [43] M. Carena, E. Ponton, J. Santiago and C. E. M. Wagner, *Electroweak constraints on warped models with custodial symmetry*, *Phys. Rev.* **D76** (2007) 035006, [[hep-ph/0701055](#)].

- [44] G. Isidori, *Flavour Physics and Implication for New Phenomena*, *Adv. Ser. Direct. High Energy Phys.* **26** (2016) 339–355, [[1507.00867](#)].
- [45] Z. Ligeti, *TASI Lectures on Flavor Physics*, in *Proceedings, Theoretical Advanced Study Institute in Elementary Particle Physics: Journeys Through the Precision Frontier: Amplitudes for Colliders (TASI 2014): Boulder, Colorado, June 2-27, 2014*, pp. 297–340, 2015. [1502.01372](#). DOI.
- [46] A. Pich, *Precision Tau Physics*, *Prog. Part. Nucl. Phys.* **75** (2014) 41–85, [[1310.7922](#)].
- [47] J. Alwall, R. Frederix, S. Frixione, V. Hirschi, F. Maltoni, O. Mattelaer et al., *The automated computation of tree-level and next-to-leading order differential cross sections, and their matching to parton shower simulations*, *JHEP* **07** (2014) 079, [[1405.0301](#)].
- [48] ATLAS collaboration, M. Aaboud et al., *Search for heavy particles decaying into top-quark pairs using lepton-plus-jets events in proton–proton collisions at $\sqrt{s} = 13$ TeV with the ATLAS detector*, *Submitted to: Eur. Phys. J.* (2018) , [[1804.10823](#)].
- [49] ATLAS collaboration, M. Aaboud et al., *Search for resonances in the mass distribution of jet pairs with one or two jets identified as b-jets in proton-proton collisions at $\sqrt{s} = 13$ TeV with the ATLAS detector*, [1805.09299](#).
- [50] ATLAS collaboration, M. Aaboud et al., *Search for additional heavy neutral Higgs and gauge bosons in the ditau final state produced in 36 fb^{-1} of pp collisions at $\sqrt{s} = 13$ TeV with the ATLAS detector*, *JHEP* **01** (2018) 055, [[1709.07242](#)].
- [51] ATLAS collaboration, M. Aaboud et al., *Search for High-Mass Resonances Decaying to $\tau\nu$ in pp Collisions at $\sqrt{s}=13\text{TeV}$ with the ATLAS Detector*, *Phys. Rev. Lett.* **120** (2018) 161802, [[1801.06992](#)].
- [52] H. Davoudiasl, J. L. Hewett and T. G. Rizzo, *Brane localized kinetic terms in the Randall-Sundrum model*, *Phys. Rev.* **D68** (2003) 045002, [[hep-ph/0212279](#)].
- [53] M. Carena, E. Ponton, T. M. P. Tait and C. E. M. Wagner, *Opaque branes in warped backgrounds*, *Phys. Rev.* **D67** (2003) 096006, [[hep-ph/0212307](#)].
- [54] PARTICLE DATA GROUP collaboration, C. Patrignani et al., *Review of Particle Physics*, *Chin. Phys.* **C40** (2016) 100001.
- [55] A. Djouadi, G. Moreau and F. Richard, *Forward-backward asymmetries of the bottom and top quarks in warped extra-dimensional models: LHC predictions from the LEP and Tevatron anomalies*, *Phys. Lett.* **B701** (2011) 458–464, [[1105.3158](#)].

- [56] D. Liu, J. Liu, C. E. M. Wagner and X.-P. Wang, *Bottom-quark Forward-Backward Asymmetry, Dark Matter and the LHC*, *Phys. Rev.* **D97** (2018) 055021, [[1712.05802](#)].
- [57] A. J. Buras, J. Girrbach-Noe, C. Niehoff and D. M. Straub, *$B \rightarrow K^{(*)}\nu\bar{\nu}$ decays in the Standard Model and beyond*, *JHEP* **02** (2015) 184, [[1409.4557](#)].
- [58] BABAR collaboration, J. P. Lees et al., *Search for $B^+ \rightarrow K^+\tau^+\tau^-$ at the BaBar experiment*, *Phys. Rev. Lett.* **118** (2017) 031802, [[1605.09637](#)].
- [59] LHCb collaboration, R. Aaij et al., *Test of lepton universality using $B^+ \rightarrow K^+\ell^+\ell^-$ decays*, *Phys. Rev. Lett.* **113** (2014) 151601, [[1406.6482](#)].
- [60] LHCb collaboration, R. Aaij et al., *Test of lepton universality with $B^0 \rightarrow K^{*0}\ell^+\ell^-$ decays*, [[1705.05802](#)].
- [61] G. Buchalla, A. J. Buras and M. E. Lautenbacher, *Weak decays beyond leading logarithms*, *Rev. Mod. Phys.* **68** (1996) 1125–1144, [[hep-ph/9512380](#)].
- [62] G. Hiller and M. Schmaltz, *Diagnosing lepton-nonuniversality in $b \rightarrow s\ell\ell$* , *JHEP* **02** (2015) 055, [[1411.4773](#)].
- [63] C. Bobeth, G. Hiller and G. Piranishvili, *Angular distributions of $\bar{B} \rightarrow \bar{K}\ell^+\ell^-$ decays*, *JHEP* **12** (2007) 040, [[0709.4174](#)].
- [64] A. Crivellin, L. Hofer, J. Matias, U. Nierste, S. Pokorski and J. Rosiek, *Lepton-flavour violating B decays in generic Z' models*, *Phys. Rev.* **D92** (2015) 054013, [[1504.07928](#)].
- [65] S. Descotes-Genon, L. Hofer, J. Matias and J. Virto, *Global analysis of $b \rightarrow s\ell\ell$ anomalies*, *JHEP* **06** (2016) 092, [[1510.04239](#)].
- [66] S. Descotes-Genon, L. Hofer, J. Matias and J. Virto, *The $b \rightarrow sl^+l^-$ anomalies and their implications for new physics*, in *51st Rencontres de Moriond on EW Interactions and Unified Theories La Thuile, Italy, March 12-19, 2016*, 2016, [[1605.06059](#)].
- [67] T. Hurth, F. Mahmoudi and S. Neshatpour, *On the anomalies in the latest LHCb data*, *Nucl. Phys.* **B909** (2016) 737–777, [[1603.00865](#)].
- [68] W. Altmannshofer, C. Niehoff, P. Stangl and D. M. Straub, *Status of the $B \rightarrow K^*\mu^+\mu^-$ anomaly after Moriond 2017*, *Eur. Phys. J.* **C77** (2017) 377, [[1703.09189](#)].

- [69] B. Capdevila, A. Crivellin, S. Descotes-Genon, J. Matias and J. Virto, *Patterns of New Physics in $b \rightarrow s\ell^+\ell^-$ transitions in the light of recent data*, *JHEP* **01** (2018) 093, [[1704.05340](#)].
- [70] F. Mahmoudi, T. Hurth and S. Neshatpour, *Updated Fits to the Present $b \rightarrow s\ell^+\ell^-$ Data*, *Acta Phys. Polon.* **B49** (2018) 1267.
- [71] J. A. Cabrer, G. von Gersdorff and M. Quiros, *Flavor Phenomenology in General 5D Warped Spaces*, *JHEP* **01** (2012) 033, [[1110.3324](#)].